



The Simplified Models Approach to Constraining Supersymmetry

Genesis Perez Rivera

► **To cite this version:**

Genesis Perez Rivera. The Simplified Models Approach to Constraining Supersymmetry. Physics [physics]. 2014. <dumas-01240903>

HAL Id: dumas-01240903

<https://dumas.ccsd.cnrs.fr/dumas-01240903>

Submitted on 9 Dec 2015

HAL is a multi-disciplinary open access archive for the deposit and dissemination of scientific research documents, whether they are published or not. The documents may come from teaching and research institutions in France or abroad, or from public or private research centers.

L'archive ouverte pluridisciplinaire **HAL**, est destinée au dépôt et à la diffusion de documents scientifiques de niveau recherche, publiés ou non, émanant des établissements d'enseignement et de recherche français ou étrangers, des laboratoires publics ou privés.



Distributed under a Creative Commons Attribution - NonCommercial - NoDerivatives 4.0 International License



UFR Sciences et Technologies



MASTER SCIENCES DE LA MATIÈRE DEUXIÈME ANNÉE

SPÉCIALITÉ : Physique des Particules

RAPPORT DE STAGE

The Simplified Models Approach to Constraining Supersymmetry

par

Genesis PEREZ RIVERA

Responsable de stage : **Dr. Suchita KULKARNI**



Juin 2014

The Simplified Models approach to constraining Supersymmetry

Genesis PEREZ RIVERA
Supervisor: Dr. Suchita Kulkarni

Abstract

The current work studies the applicability of Simplified Model Spectra (SMS) framework to Supersymmetric (SUSY) scenarios.

The SMS framework is useful as it involves a small number of parameters and presents the experimental results for SUSY searches in a general way. The SMS framework does not depend on a particular theory, therefore it is useful for a generic re-interpretation and test of scenarios.

To use the SMS framework to constraint the SUSY parameter space, two automated tools were used: SModelS and Fastlim. The accomplishment of both tools, just as the strengths and limitations are remarked in this work.

Finally, it was taken a specific SUSY scenario -Natural SUSY (NSUSY) and analyzed using both SModelS and Fastlim. As a result, it is shown that it is possible to constrain NSUSY scenarios within the SMS framework, but, to reach a more generic interpretation of the parameter space, improvements in both codes are needed.

Résumé

Ce travail étudie l'applicabilité du cadre Simplified Model Spectra (SMS) aux scénarios supersymétriques (SUSY).

SMS est utile car il implique un petit nombre de paramètres et présente les résultats des recherches en SUSY de façon générale. Pour utiliser le cadre sms afin de contraindre l'espace des paramètres supersymétriques.

Deux outils numériques ont été utilisés : SModelS et Fastlim. Les résultats comparatifs de ces deux outils numériques sont effectuées dans ce travail.

Enfin, un scénario supersymétrique spécifique -Natural SUSY (NSUSY)- a été analysé en utilisant à la fois SModelS et Fastlim. Il est alors montre qu'il est possible de contraindre les scénarios NSUSY dans le cadre de SMS, mais pour une meilleure interprétation les deux codes doivent être améliorés.

Contents

Introduction	4
1 Supersymmetry	5
1.1 The open questions of the SM	5
1.2 The Minimal Supersymmetric Standard Model	5
1.3 Natural SUSY	7
2 Simplified Model Spectra	8
2.1 The Simplified Model Spectra, SMS	8
2.2 SMS example	9
2.3 SMS upper limits and interpretations	9
3 The Re-interpretation tools	10
3.1 SModelS and Fastlim	11
4 SModels and Fastlim: a first comparison	14
4.1 Arbitrary SUSY models: SMS decomposition examples	14
5 Natural Supersymmetry SMS interpretation	19
5.1 Setup of the study	19
5.2 Constraining the parameter space: excluded points from the mass spectrum	20
5.2.1 $\tan [\beta] = 10$	20
5.2.2 $\tan [\beta] = 50$	22
6 Conclusions	23
A Nomenclature	25
B List of SUSY Analyses implemented	26
C SMS decomposition examples	29
D Auxiliary Plots	31

Introduction

The Standard Model (SM) of particles is one of the successful theories in physics: so far, all its particles have been found (including possibly the Standard Model Higgs) and up to electro-weak energies they behave as predicted; one could say that it describes nearly all known phenomena in particle physics. Nevertheless, there are still questions (Section 1.1) to be answered and understood, which points towards the necessity of a greater description of nature and it remains to be discovered. For instance, the recent discovery of a Higgs-like particle with mass around 125 GeV makes the question of stability of the electroweak scale (known as the hierarchy problem) even more imminent.

Different scenarios have emerged as an extension of the SM during the past decades, explaining one or more open questions. One of them is Supersymmetry (SUSY), which is one of the largely hunted scenario at the Large Hadron Collider (LHC) at CERN. The supersymmetric extension of the SM, which adds the minimum extra particle content, is called the Minimal Supersymmetric Standard Model (MSSM) (Section 1.2), and it agrees with the SM philosophy, as an enlarged symmetry of the Poincaré symmetry.

As a result, supersymmetric signatures¹ have been searched by the ATLAS and CMS collaborations using data from proton-proton collisions at 7 TeV and 8 TeV, but without great success. This has led to question about which SUSY model² would be discovered at the experiments if at least one signature is found.

In the interpretation of the experimental results of the LHC, many of the current limits on the SUSY particles are based on model assumptions, which impose particular relations between the masses, branching ratios, etc. [1]. In fact, ATLAS and CMS present their results only in particular slices of the parameter space of a few models. Consequently, these interpretations are model dependent, or in other words, the conversion of number of events to limits on masses, involve assumptions which inherently bring model dependence. Therefore, the searches are providing sort of limited constraints on SUSY, which could be just a small part of the complete MSSM parameter space.

For example, the collaborations have been using, for the interpretation of their results, a model called the Constrained Minimal Supersymmetric Standard Model (CMSSM) [2], which is characterized by just four-and-a-half parameters. The interpretation of the search results within this model is interesting, because it provides (for example, and up to certain degree) an easy way to compare limits on reaches or show performances. However, it is computationally very demanding and it risks to impose unjustified constraints on SUSY, that might be not covered in the CMSSM.

Another different phenomenological approach is called the phenomenological MSSM (pMSSM)[3], which uses a 19-dimensional parametrization of the MSSM and it constraints the SUSY particles with as few simplifying assumptions as possible, with a larger set of predictions for the properties of SUSY partners, but still covering only some slices of the parameter space.

Driven by the necessity of trying to constrain as many models as possible and to have a more generic interpretation approach of the SUSY parameter space, the collaborations at the LHC have adopted the Simplified Model Spectra (SMS) (Section 2): a simplified model framework that does not depend on a particular SUSY model, but that has been inspired by the phenomenological similarities between all of them. Alike phenomenology predicted by different SUSY models sharing similar topologies³.

¹A *signature* is a qualitative specification of a final state. For example, leptons and photons.

²A fully specified theory

³A *topology* is a fully specified production mode and decay chain. For example, a supersymmetric gluon (gluino) decaying into a supersymmetric neutral gauge particle(neutralino) and two jets.

1 Supersymmetry

1.1 The open questions of the SM

Despite the fact that the SM is a successful theory, which gives a good description of nearly all the phenomena in particle physics, it seems to be incomplete when looking at some fundamental questions and finding no satisfactory answer. Some of the following problems have impelled to look in possible scenarios Beyond the Standard Model (BSM).

1. There are nineteen free parameters in the SM, which can only be experimentally measured. Therefore, it results unsatisfactory to believe that these parameters can only be determined by measurement, instead of a theory that could predict them.
2. $U(1)_Y \otimes SU(2)_L \otimes SU(3)$ local invariance gives a very good match between theory and experiment, but there is none explanation for this choice.
3. More families could exist interacting according to the SM. Why are they only three families? Why is the pattern for 1 generation replicated 3 times? In general terms, no limits can be set on the numbers or masses of quarks and leptons.
4. The unification of the electroweak and QCD couplings; they could be unified into a simpler structure.
5. The gravitation does not seem to fit in the SM, although it is a fundamental interaction.
6. Nearly 4% of our Universe is made up of matter particles. The question about what is our Universe made up has led to a dark matter (DM) scenario. Yet its abundance in the Universe, the SM does not offer candidates to explain the DM observations.
7. The electroweak symmetry is a powerful one in the SM, yet it fails in the description of the particle masses due to local gauge invariance. Thus it is needed a mechanism that gives mass to massive particles and that keeps massless the non-massive ones. This mechanism introduces a scalar sector in the electroweak unification and it breaks spontaneously the symmetry, by choosing a vacuum value. The scalar sector is introduced by a scalar field, called the Brout-Englert-Higgs boson, and it could be understood as a fluctuation of the vacuum.

Despite the vacuum value can be determined from low energy physics results⁴, the mass of the Higgs boson has been a “free parameter” of the theory. The Higgs mass, m_H^2 , receives enormous quantum corrections, especially from the heaviest particles. The most important are coming from the fermionic couplings $\lambda_f H \bar{f} f$ and it will be something like [4]:

$$\Delta m_H^2 = \frac{|\lambda_f|^2}{8\pi^2} \Lambda_{UV}^2 + \dots$$

where Λ_{UV} refers to the ultraviolet cut-off, and it brings with itself some physical interpretation that cannot be neglected. But, a new difficulty is introduced, if it is desired to have a valid description of the physics above the Planck scale, it will be necessary to find a symmetry that protects the Higgs mass and that includes new terms to cancel the divergence.

1.2 The Minimal Supersymmetric Standard Model

Symmetries play a crucial role in physics. Symmetry groups as the Poincaré group, consisting of Lorentz transformations and translations in the Minkowski space-time, are very successful in describing particle interactions. Thus it could be interesting to question if it is possible to extend this symmetry group, in

⁴The vacuum value is $v = 256$ GeV.

order to have a better description of nature. The only way to do it, it is with a non-trivial product of the Poincaré algebra with an internal symmetry, such as a gauge symmetry[5]. This is the basic principle of supersymmetry (SUSY).

SUSY is a symmetry which relates fermions and bosons, using a transformation that turns bosonic states into fermionic states, and vice versa[4, 6]. It must then exist an operator, Q , such that

$$\begin{aligned} Q|\text{Boson} \rangle &= |\text{Fermion} \rangle, \\ Q|\text{Fermion} \rangle &= |\text{Boson} \rangle. \end{aligned} \tag{1}$$

This operator Q must be an anticommuting spinor. Its hermitian conjugate Q^\dagger , together with Q , are symmetry generators; that means, they satisfy an algebra of anticommutation and commutation relations:

$$\begin{aligned} \{Q, Q^\dagger\} &= P^\mu \\ \{Q, Q\} &= \{Q^\dagger, Q^\dagger\} = 0 \\ [P^\mu, Q] &= [P^\mu, Q^\dagger] = 0 \end{aligned}$$

where P^μ is the four-momentum generator of space-time translations[4, 6].

But increasing the symmetry from the Poincaré group to a super-Poincaré group, it is also to increase the coordinate space from Minkowski space (with x^μ coordinates), to a superspace with coordinates of the kind $X = (x^\mu, \theta^\alpha, \bar{\theta}^{\dot{\alpha}})$ [5], where each of the components is a field. Hence, X is going to be a superfield with several fields together.

Even so, if the desired SUSY extension of the SM is the simplest one, where one introduces only those couplings and fields necessary for consistency, only three basic superfields will survive[5, 7]:

- The Field containing the gauge bosons and their fermionic partners, the gauginos
- The field containing the fermions and their scalar partners
- The Higgs scalar boson

They correspond to the minimal extension of the SM, the Minimal Supersymmetric Standard Model (MSSM), and their field content[5] is shown in Table 1 and Table 2.

	Superfield	spin 0	spin $\frac{1}{2}$	$(SU(3), SU(2), U_Y(1))$
squarks and quarks	Q	$(\tilde{u}_L, \tilde{d}_L)$	(u_L, d_L)	$(3, 2, \frac{1}{6})$
	U	\tilde{u}_R^\dagger	\tilde{u}_R^\dagger	$(\bar{3}, 1, -\frac{2}{3})$
	D	\tilde{d}_R^\dagger	\tilde{d}_R^\dagger	$(\bar{3}, 1, \frac{1}{3})$
sleptons and leptons	L	$(\tilde{\nu}, \tilde{e}_L)$	(ν, e_L)	$(1, 2, -\frac{1}{2})$
	E	\tilde{e}_R^\dagger	\tilde{e}_R^\dagger	$(1, 1, 1)$
higgs and higgsinos	H_u	(h_u^+, h_u^0)	$(\tilde{h}_u^+, \tilde{h}_u^0)$	$(1, 2, \frac{1}{2})$
	H_d	(h_d^0, h_d^-)	$(\tilde{h}_d^0, \tilde{h}_d^-)$	$(1, 2, -\frac{1}{2})$

Table 1: Chiral superfields of the MSSM and the particle content.

	Superfield	spin 0	spin $\frac{1}{2}$	$(SU(3), SU(2), U_Y(1))$
gluinos and gluons	G	\tilde{g}	g	$(8, 1, 0)$
winos and W-bosons	W	$(\tilde{W}^\pm, \tilde{W}^0)$	(W^\pm, W^0)	$(1, 3, 0)$
bino and B-boson	B	\tilde{B}	B	$(1, 1, 0)$

Table 2: Vector superfields of the MSSM and the particle content.

As the SUSY extension of the SM is the minimal, the gauge interactions are determined by the gauge group in the same way as in the Standard Model: $SU(3)_V \times SU(2)_L \times U(1)_Y$ (shown in the Tables 1 - 2). Keeping in mind this principle, to build a model only with the necessary terms, the superpotential of the Lagrangian of the MSSM[5, 7] is:

$$W = \sum_{i,j}^3 \sum_{a,b}^2 \left[(y_u)_{ij} U^i Q_a^j \epsilon^{ab} (H_u)_b - (y_d)_{ij} D^i Q_a^j \epsilon^{ab} (H_d)_b - (y_e)_{ij} E^i L_a^j \epsilon^{ab} (H_d)_b \right] + \mu H_u H_d \quad (2)$$

where $i, j \in 1, 2, 3$ label the family/flavour; $a, b \in 1, 2$ are SU(2) labels; the ϵ^{ab} is used to make, for example the term QH_d , a singlet under SU(2) and to have finally a whole term SU(2) gauge invariant. The terms y_u , y_d and y_e are dimensionless Yukawa couplings giving rise to quark and lepton masses. Finally, the last factor is given by

$$H_u H_d \equiv \epsilon^{ab} H_{ua} H_{db} = H_u^0 H_d^0 - H_d^+ H_u^- \quad (3)$$

Then, the Lagrangian is

$$\mathcal{L}_{SUSY} = - \left[\sum_{j,k} \frac{\partial^2 W}{\partial \phi_j \partial \phi_k} \psi_j \psi_k + \text{h.c.} \right] - \sum_j \left| \frac{\partial W}{\partial \phi_j} \right|^2 \quad (4)$$

where ϕ_i are scalar and ψ_i fermion fields; W only depends on the scalar fields.

In this description of MSSM, each of the SM particles would have a superpartner with same mass but differ spin, unless some spontaneous breaking in the theory. To avoid a clear contradiction to the observations, and in order to have a realistic description of the SM in a supersymmetric extension, SUSY must be broken in a way that will assure superpartners to have a larger masses. But, the breaking must be done such that the features of the symmetry are not lost.

It is then considered a "soft" supersymmetry breaking. That means that the effective Lagrangian of the MSSM could be rewritten as,

$$\mathcal{L} = \mathcal{L}_{SUSY} + \mathcal{L}_{soft} \quad (5)$$

But, the breaking procedure is not straightforward, so the manner of proceed is by introducing a hidden sector, then to break SUSY in that sector and to mediate the consequences in the visible one. This mechanism, and the mediation to compute the induced breaking in the visible sector, are still unknown. The solution so far has been to parametrize the space, to introduce the breaking terms by hand (according with the different models of SUSY breaking) and try to measure this parameter space, waiting for a consistent picture that agrees with any of the SUSY breaking possible scenarios.

1.3 Natural SUSY

Due to the problem of hierarchy in the SM, it seems necessary to find a valid description for the particle interactions above $\sim 10^3$ GeV. Therefore, if there are any SUSY partner particles, it is natural that they show up around this order, or in other words, their masses should be not so far from $\sim 10^3$ GeV.

If SUSY is broken spontaneously, there should exist a similar mechanism to the electroweak breaking symmetry (EWBS) of the SM. In fact, the ordinary Higgs mechanism in gauge theories have an analogous in SUSY, called the super-Higgs mechanism[7].

Likewise the SM, to achieve a natural EWBS in the MSSM, the contributions to the quadratic terms of the Higgs potential in SUSY must be around the order of the vacuum value⁵. Consequently, each contribution Δm_H^2 to the Higgs mass should be less than or of the order of m_H^2 , to avoid fine tuning over each term to cancel each other.

⁵Remember that $v \sim 246$ GeV.

This naturalness requirement could be summarized by the EWBS condition[8],

$$-\frac{m_Z^2}{2} = (m_{H_u}^2 + |\mu|^2) \quad (6)$$

in the MSSM, where μ term is included in the Higgsino mass at the tree level, m_{H_u} is the soft mass of the up-type Higgs and m_Z the Z-boson mass at the electroweak scale.

The Higgs potential in a SUSY theory is also unstable to quantum loop corrections, and it is corrected by both gauge and Yukawa interactions. Thus it is required some naturalness in SUSY: weakly-interacting physics at TeV scale or below must exist.

This naturalness states the following: the relevant terms contributing to the quantum loop corrections over the Higgs potential pose bounds on the supersymmetric spectrum.

First, as the m_H^2 includes the μ term, higgsinos must be light because their mass is going to be directly controlled by μ . Then, the largest contribution to the Higgs potential comes from the top-stop loop[8], therefore an upper bound is set on the stop masses. However, as the stop left handed is a doublet, which includes the sbottom left handed, the latter must also has an upper bound.

The gluino, which introduces a large correction to the top squark masses at first loop, and therefore into the Higgs potential at second loop.

In summary, the minimal requirements for a natural SUSY spectrum are[8] (Figure 1:

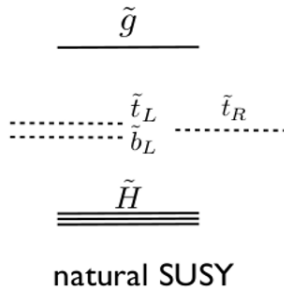


Figure 1: Natural SUSY spectrum [8]

- at least one stop and possibly left-handed sbottom, both below 500-700 GeV.
- two higgsinos: one chargino and two neutralinos below 200-300 GeV. In the absence of other chargino/neutralinos, their spectrum is quasi-degenerate.
- a not too heavy gluino, below 900 GeV-1.5 TeV

2 Simplified Model Spectra

2.1 The Simplified Model Spectra, SMS

The SMS is an effective-Lagrangian description of the BSM interactions, involving a small number of new particles and it is represented by a small number of parameters[9]. All the properties of a given BSM model are reduced to its mass spectrum, the production cross section (σ) and the decay branching ratios (BR). The SMS offers a generic framework to understand the implications of *new-physics* searches.

In the SMS considered in this work, only the productions process for two primary particles is taken: each primary particle can undergo to a direct decay or to a cascade decay through an intermediate new particle. This work studied only SUSY models where each particle decay chain will end with a neutral, undetected particle, denoted the Lightest Supersymmetric Particle (LSP), mainly because the current SMS results available from the LHC are for SUSY signatures with missing (transverse) energy (MET).

2.2 SMS example

Every SMS interpretation is based on a set of assumptions and is applicable for specific topologies. A generic point in the theory parameter space contains many different topologies and it is sensitive to more than one SMS analysis. However, the SMS decomposition does not depend on characteristics of the SUSY particles (as spin, chirality), yet of the masses and final states.

Let us consider a SUSY particle decay with jets plus MET final state, for example a top squark (\tilde{t}) decay, as shown in Figure 2. For this example, the neutralino $\tilde{\chi}_1^0$ is considered to be the LSP (or $\tilde{\chi}_{LSP}$).

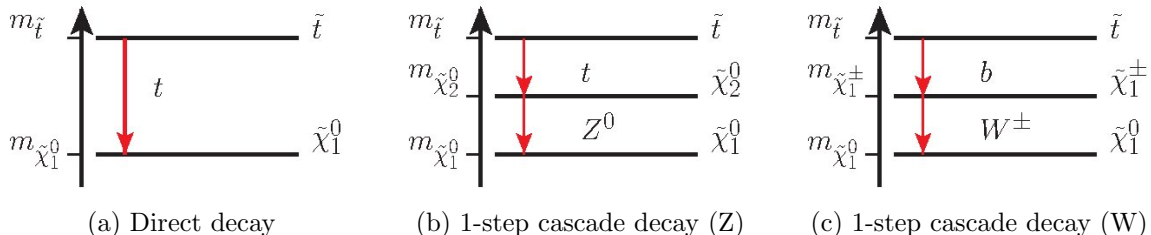


Figure 2: The three top squark simplified models discussed in the example.

One of the possible topologies is the 2-body direct decay, $\tilde{t} \rightarrow \tilde{\chi}_1^0 t$, where the sparticle is going directly to the expected final state (Figure 2a). But this is not the only possible topology that could be considered, the sparticle could have a one-step cascade decay and it will go to an intermediate particle (for instance, a heavier electroweakino). In this example, the top squark decays to a chargino that subsequently decays to a gauge boson and the LSP (Figure 2c) - $\tilde{t} \rightarrow b (\tilde{\chi}_1^\pm \rightarrow) W^\pm \tilde{\chi}_1^0$, or it is going to a heavier neutralino that decays to a neutral gauge boson and the LSP (Figure 2b) - $\tilde{t} \rightarrow t (\tilde{\chi}_2^0 \rightarrow) Z^0 \tilde{\chi}_1^0$. Both, W and Z hadronic decays contribute to the same final state of a stop decaying to jets + MET.

Now, as the SMS is described by the masses spectrum and the production cross sections, this example will be parametrized by the respective cross section $\sigma(pp \rightarrow \tilde{t}\tilde{t} + X)$, the masses $m_{\tilde{\chi}_{LSP}} - m_{\tilde{t}}$ and the mass of the intermediate particle, m_{int} , when a cascade decay is considered.

The choice of an intermediate particle alters the kinematics of the theory and it is useful to consider a family of “mass slices”[10] for the intermediate particle. For the example here considered, a family of chargino mass slices will be determined by

$$m_{\chi^\pm} = m_{\chi_{LSP}} + x(m_{\tilde{t}} - m_{\chi_{LSP}}). \quad (7)$$

Here the value of x describes the kinematics in the decays: intermediate values of x cover a variety of kinematics; for instance, in hadronic searches, the limit of a small x approaches the direct decay[10].

2.3 SMS upper limits and interpretations

For each final state, two procedures can be used to establish SMS limits, which will allow to confront the theoretical predictions against the experimental results from the collaborations. One of the possibilities, it is to use the number of events in each signal region as reported by the experiments and reconstruct the theoretical number of events by using efficiency maps. While the other one consists to establish an upper limit (UL) on the $\sigma \times \text{BR}$, assuming a specific topology contribution to the entire final state.

These limits will admit a generic interpretation of the experimental results independently of the model and all the information is coming directly from the experiments.

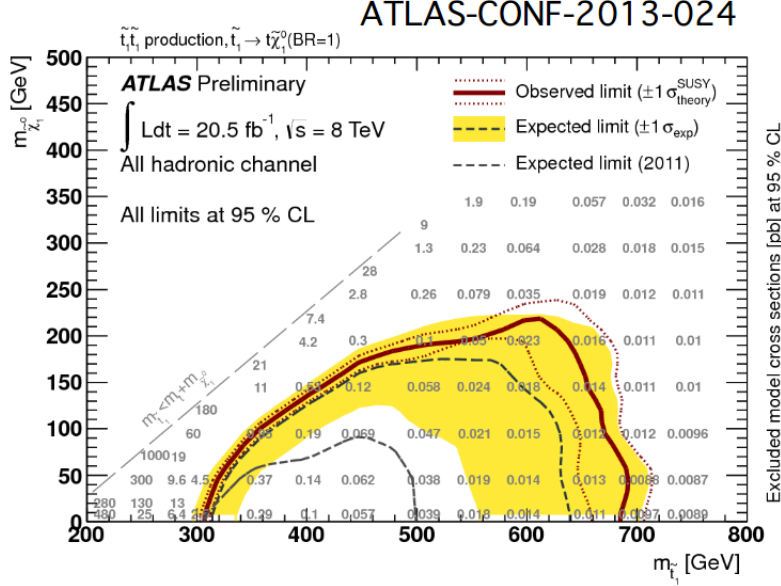


Figure 3: The SMS upper limits, all the information comes directly from the experimental results. In this example, from the ATLAS experiment [11].

For example, the figure 3 represents the SMS $\sigma \times BR$ limits from a search for direct production of the top squark in all-hadronic $t\bar{t} + \text{MET}$ final state for the UL, for $\tilde{t}_1 \rightarrow t\tilde{\chi}_1^0 (BR = 1)$ decay chain [11]; and it could be understood in the following way: the experimental exclusion limits have been placed in this model of top squark pair production, followed by the decay $\tilde{t}_1 \rightarrow t\tilde{\chi}_1^0$ with 100% BR considered. The results observed by ATLAS collaboration are consistent with SM expectations [11]. Then, the top squark is excluded with masses between 300 GeV and around 700 GeV, for a nearly massless LSP up to 250 GeV mass. The plot shows the expected and observed exclusion limits at 95% CL.

These numbers in the plot are the experimental limit for the $\sigma \times BR$ value, where the analysis is considered to be sensitive only to one decay channel. However, this limit is used to exclude (or allow) a theoretical SMS topology with the same final state and production, but including different chains. The question would be, is the theoretical $\sigma \times BR$ of certain model, for a given mass combination, larger than the number shown in the plot? If the answer is affirmative the combination and channel will be excluded, while if negative it will be allowed.

3 The Re-interpretation tools

The main idea of the approach described before falls on the re-interpretation and understanding of the experimental results obtained by the collaborations. But, let us consider three leptons + MET final state. In fact, there could be different topologies contributing to this final state, thus the signature could be produced by different particles with different decay chains. So, would it be possible to choose a dominant topology that will describe in a better way the final state results? What happens with the rest of the topologies? Are they still contributing? How large is their contribution?

Experimentally, it is often chosen a dominant topology (each BR is assumed to be 100%), while the others are forbidden.

But, not only it is useful to have a better and more complete interpretation of the final state, trying to confront as many theories and topologies as possible with the experimental results, just as the SMS approach does; it will also be advantageous to have a centralized database of all the SMS results available to check a SUSY point against these experimental results. As a result, tools have been designed to

decompose the signal of a spectrum into SMS topologies and to test it against the bounds in the LHC, in order to get a richer picture of the parameter space.

3.1 SModelS and Fastlim

- **The re-interpretation tools:** The following tools, as it was stated, decompose the signal of a SUSY spectrum⁶ into SMS topologies and test them against all the existing bounds at the LHC, in the SMS context. The idea is to build up a database of experimental SMS results in the interpretation of SUSY models and to apply them to the models interpretations.

SModelS re-interpretation tool [9]: SModelS decomposes the full BSM spectrum to a set of SMS topologies. The decomposition is generic and can be applied to any scenario apart from SUSY. It computes the respective weights ($\sigma \times BR_{th}$) and it confronts the theoretical prediction with the experimental results. Moreover, all the important information from any spectra of arbitrary complexity is reduced to three main objects: *the diagram topology*, which gives the number of vertices and SM final state particles in each of them; *the masses of the BSM particles* appearing and *the diagram weight*.

Fastlim re-interpretation tool [12]: It also uses the simplified models, however, it aims only at SUSY scenarios (the decomposition is done under consideration of natural SUSY topologies). It was designed to consider a traditional “recasting” approach or, in other words, cut-and-count regions, just as the defined by the experiments, where the predicted events by the theory are confronted with the observed data in the signal regions. Thus the idea is to have a tool that uses an interpolation of pre-calculated efficiency and cross section tables, instead of reconstructing the visible cross sections by Monte Carlo (MC) simulation.

- **The inputs:** For SModelS, the information needed is the spectrum file and the decay table, the production cross sections are theoretically computed. On the other hand, Fastlim uses input masses and the decay branching ratios of the SUSY particles, while information as the cross sections or the efficiency maps are predefined, tabulated and provided by the tool.

For SModelS, the user has the possibility to control certain parameters and characteristics (as the value of the mass splitting for the particles defining invisible decays, the inclusion of the topologies description in the output files and some other features), with the help of a *parameters input file* given. While for Fastlim, none of these options is still available.

- **The methodology:**

SModelS:

- A SLHA file containing BR or an LHE file is read.
- The diagram weight for each topology is computed by SModelS (as shown in the Figure 4). From this point, there will not longer be any reference to the specific details of the model [9].
- These theoretical predictions obtained from the decomposition will be confronted with the experimental constraints: the signal topologies produced in the decomposition are mapped to the SMS topologies constrained by data. The signal topologies are combined according to the assumptions of each experimental result. This will allow to directly compare the theoretical prediction with the experimental UL and to decide if a parameter point is allowed or excluded.

⁶Initially it has been used only with SUSY models, but it can be extended to any other BSM scenario as soon as the experimental results allow it.

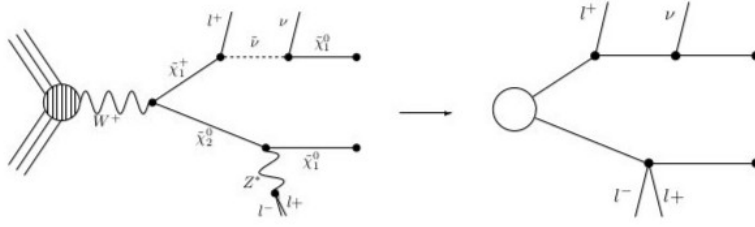


Figure 4: Decomposition of a full model diagram into its SMS equivalent topology, figure taken from [9].

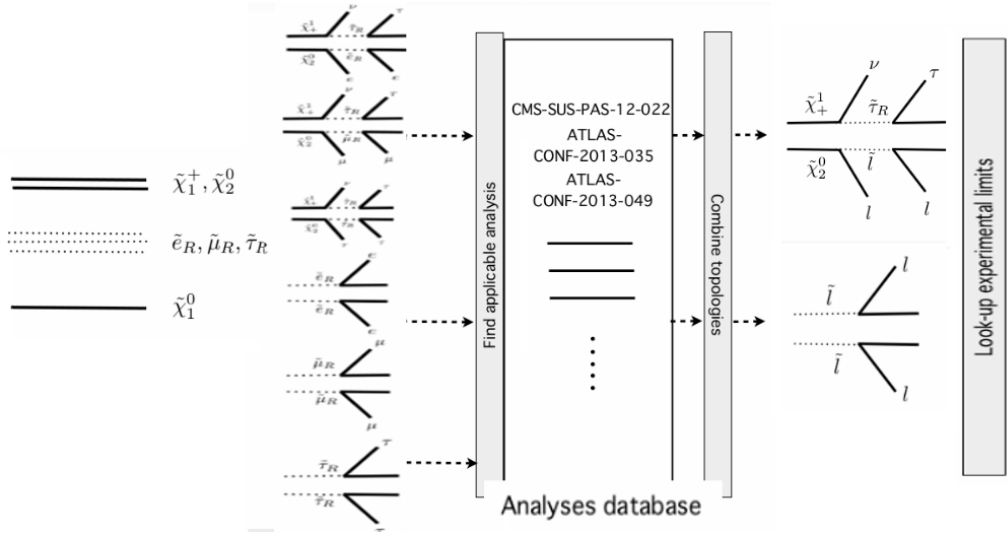


Figure 5: SModelS methodology [13].

- A convenient measure for exclusion is taken: the ratio between the theoretical prediction of the diagram weight and the experimental result from the UL, given by the experimental analysis,

$$R = \frac{\sigma \times \text{BR}_{\text{th}}}{(\sigma \times \text{BR})_{\text{exp}}^{\text{UL}}} \quad (8)$$

If this ratio $R > 1$ for a particular BSM spectrum, it will be excluded.

Fastlim:

- The SLHA input file is read.
- Fastlim will go through all the decay chains and it will extract the masses and branching ratios information from the input file.
- To confront the theoretical prediction of the number of events with the limits in the same signal region, the tool will also look for an exclusion ratio, given by the theoretical contribution to the signal region, $N_{\text{SUSY}}^{(a)}$, and the experimental report by the collaborations N_{UL} , according with the following expression:

$$R^{(a)} \equiv N_{\text{SUSY}}^{(a)} / N_{\text{UL}}. \quad (9)$$

The theoretical contribution depends generally on the sparticle mass spectrum and the couplings, and it can be written as[12]:

$$N_{SUSY}^{(a)} = \sum_i^{all\ topologies} \epsilon_i^{(a)} (\sigma \times BR)_i L_{int} .$$

(1) (2) (3) (4) (5)

- (1) Theoretical contribution
- (2) Contribution of all event topologies for the signal region
- (3) Efficiency
- (4) Inclusive cross section
- (5) Integrated luminosity

The efficiency $\epsilon_i^{(a)}$ is estimated with MC simulation and it will depend only on the masses and couplings of the particles appearing in the Fastlim topology. The efficiency is pre-calculated and tabulated for short decay chains, that means topologies with two or three different SUSY particles [12]. Then, $\epsilon_i^{(a)}$ is obtained by interpolation. The cross section for a specific topology, σ_i , is written as the product of the production cross section and the branching ratios for the decay chains. Similarly to the efficiencies, Fastlim has tabulate cross sections for different production modes.

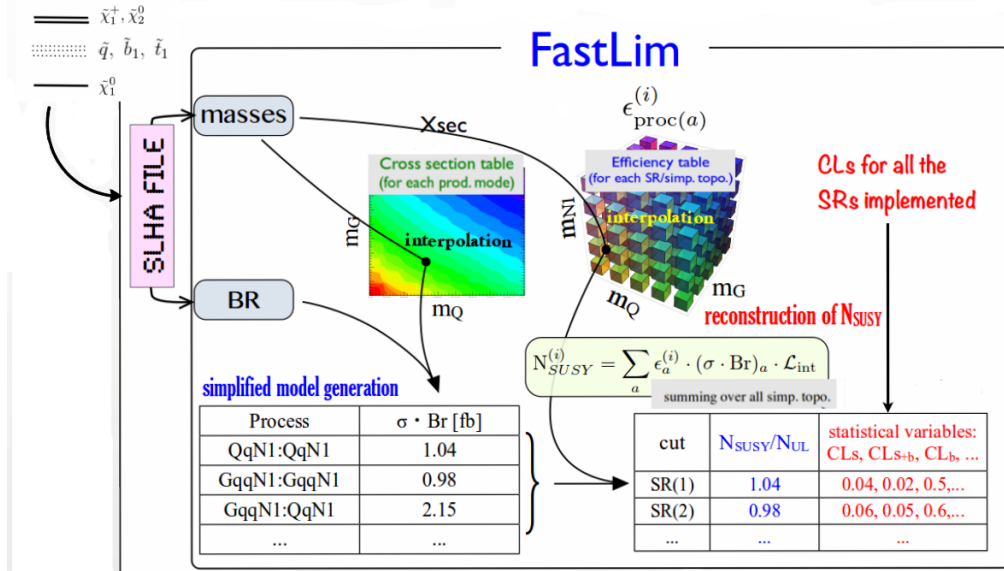


Figure 6: Fastlim methodology [14].

- The production cross sections are extracted from the tables and the presence of the efficiency tables is checked for the topologies under consideration (see Figure 6). Thus, the visible cross section for the topologies can be computed by multiplying the cross section and the efficiency. All the information necessary to set a limit in the signal region is retrieved: if the ratio in the equation 9 is larger than the unit (> 1) for a particular BSM spectrum, this is excluded.

- **Topology definitions:**

SModels:

For SModels, the topologies are classify according to the number of vertices in each branch and which particles are appearing. The topologies will be explicitly written as shown in the Figure 7. However, the labeling used in the output summary file is given, in first instance, by the SMS topologies naming shortly described before. All the particles chains that will be considered end with the LSP, and they are explained in detail in the Table 8.

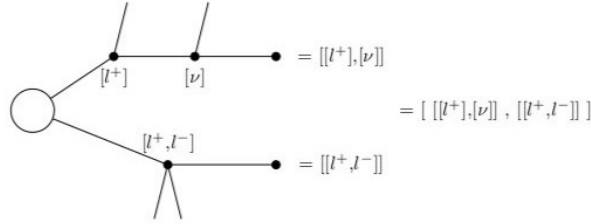


Figure 7: *The labeling scheme adopted by SModelS, figure taken from [9].*

Fastlim:

Each event topology has a name assigned in a simple way: each string identify unambiguously a SMS topology: the mother SUSY particle is written firstly; it is followed by the sequences of intermediate on shell particles, in other words, the SM are placed right after their mother, but in alphabetic order, followed by the SUSY daughter. Finally, each string in the production is connected with a “_” in between, as shown in figure 8.

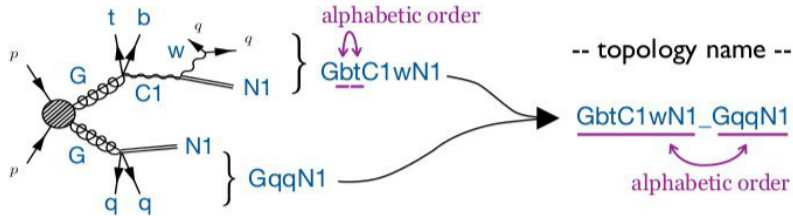


Figure 8: *Naming scheme for the event topology, figure taken from [12].*

4 SModelS and Fastlim: a first comparison

So far, a brief description of the characteristics of both tools has been made. It is useful to make a comparison between their re-interpretation of any SUSY model spectrum, and to observe the possible differences between their results even when they are decomposing in the same slice of the parameter space. As a result, it would be possible to answer questions about their behaviour: are both having a similar phenomenological description? Are there any considerable differences in the exclusion of a mass configuration spectrum? Or are they interpreting it in the same way? Why? Are they losing information when considering one of the tools but not the other? The search for the answer of these questions would be useful not only to estimate the accomplishment of both frameworks, but also to find the strong points and weakness of both, and try to find if there is something that could be done to improve the SMS automated decomposition, and get a more generic and better description of the parameter space in terms of SMS approach.

In this part, results from Fastlim and SModelS for a set of SUSY points are compared.

4.1 Arbitrary SUSY models: SMS decomposition examples

Three SLHA files were taken, each of them with a different mass spectrum configuration, and analysed by SModelS and Fastlim. The Table 3 shows the list of analyses implemented from the database (the

database analyses is described in the Appendix B) by both and it tells if the configuration is excluded or not when compared with the experimental bounds (with the exclusion ratio).

Analysis	SModelS exclusion ratio	Fastlim exclusion ratio
Point 1		
light \tilde{q} , $\tilde{\chi}_{1,2}^0$, $\tilde{\chi}_1^\pm$, $\tilde{t}_{1,2}$, \tilde{b}_1 , \tilde{g}		
ATLAS_CONF_2013_035	<1	<1
ATLAS_CONF_2013_053	<1	<1
ATLAS_CONF_2013_048	<1	<1
ATLAS_CONF_2013_037	<1	<1
ATLAS_CONF_2013_062	<1	<1
ATLAS_CONF_2013_047	>1 Excluded!	<1
Point 2		
light \tilde{q} , $\tilde{\chi}_{1,2}^0$, $\tilde{\chi}_1^\pm$, \tilde{t}_1 , \tilde{b}_1 , \tilde{g}		
ATLAS_CONF_2013_024	<1	<1
ATLAS_CONF_2013_035	<1	<1
ATLAS_CONF_2013_037	<1	<1
ATLAS_CONF_2013_047	>1 Excluded!	<1
ATLAS_CONF_2013_048	<1	<1
ATLAS_CONF_2013_053	<1	<1
ATLAS_CONF_2013_062	<1	<1
Point 3		
light \tilde{q} , $\tilde{\chi}_{1,2}^0$, $\tilde{\chi}_1^\pm$, \tilde{t}_1 , \tilde{g}		
ATLAS_CONF_2013_062	<1	<1
ATLAS_CONF_2013_047	>1 Excluded!	<1
ATLAS_CONF_2013_048	<1	<1

Table 3: Analyses implemented by Fastlim and SModels in the first group of points and their exclusion ratio.

As it was described before, for SModelS the exclusion ratio tells if, for each individual topology considered, the theoretical prediction is fitting -or not- within the experimental bounds for the mass spectrum considered. While for Fastlim the exclusion ratio implies the addition of all the topologies (between the theoretical contribution and the experimental report) for a signal region; then, if one of those regions taken has a ratio larger than the unit, the configuration is excluded for that analysis.

Now, one would expect that if SModelS excludes certain configuration, Fastlim will do it too, yet when looking into the Table 3, one notices that it is not exactly what takes place for the analysis ATLAS_CONF_2013_047[15]. Actually, it would be necessary to analyse deeply the mass spectrum configuration of each file and the considerations taken by both tools when the theoretical prediction and the experimental results were confronted, to understand what happened.

Point 1

Let us start with the interpretation of the mass spectrum and the theoretical expectations for it. All the information that could be needed is found in the SLHA file.

Here, the mass spectrum kinetically allows the production of 1st and 2nd generation squarks, the two mass eigenstates for the bottom squark, \tilde{b}_1 and \tilde{b}_2 , and the lightest top squark mass eigenstate, \tilde{t}_1 . It also allows the production of the two lightest neutralinos, $\tilde{\chi}_{1,2}^0$; the gluino, \tilde{g} , and the lightest chargino, $\tilde{\chi}_1^\pm$.

The neutralino mixing matrix states that the lightest neutralino ($\tilde{\chi}_1^0$) is bino like, while the second neutralino ($\tilde{\chi}_2^0$) is wino like. From the squark mixing matrices, it is possible to infer that the \tilde{t}_1 and \tilde{b}_1

squarks are mainly left-handed squarks.

Based on this information (mass spectrum and mixing matrices), it is possible to deduce nearly the decays and topologies which will be more probable within this configuration, as shown below (where the most probables are at the beginning of the lists):

$$\begin{array}{cccc}
 \tilde{\chi}_1^\pm \rightarrow \tilde{\chi}_1^0 W^\pm & \tilde{b}_1 \rightarrow \tilde{\chi}_1^+ t & \tilde{t}_1 \rightarrow \tilde{\chi}_1^+ b & \tilde{b}_2 \rightarrow \tilde{\chi}_1^0 b \\
 \tilde{\chi}_2^0 \rightarrow \tilde{\chi}_1^0 Z & \tilde{b}_1 \rightarrow \tilde{\chi}_2^0 b & \tilde{t}_1 \rightarrow \tilde{\chi}_2^0 t & \tilde{b}_2 \rightarrow \tilde{\chi}_2^0 b \\
 & \tilde{b}_1 \rightarrow \tilde{\chi}_1^0 b & \tilde{t}_1 \rightarrow \tilde{\chi}_1^0 t & \tilde{b}_2 \rightarrow \tilde{\chi}_1^+ t \\
 & & & \tilde{b}_2 \rightarrow \tilde{t}_1 W
 \end{array}$$

Possible decays for the mass spectrum.

Subsequently, it is possible to compare the expected sparticle production and decays for those topologies obtained from the SMS decomposition done by both tools. These are listed in the Table 4 (the naming convention here use is described in Appendix A), with no particular order (the number indicates the corresponding topology figure).

SModelS	Fastlim
TChiWZon (10)	B2bN1_B2bN1 (9a)
T2bb (9a)	B1bN1_B1bN1 (9a)
T6bbWW (9b)	T1tN1_T1tN1 (9a)
T6WW (9b)	

Table 4: Topologies implemented by SModelS and Fastlim.

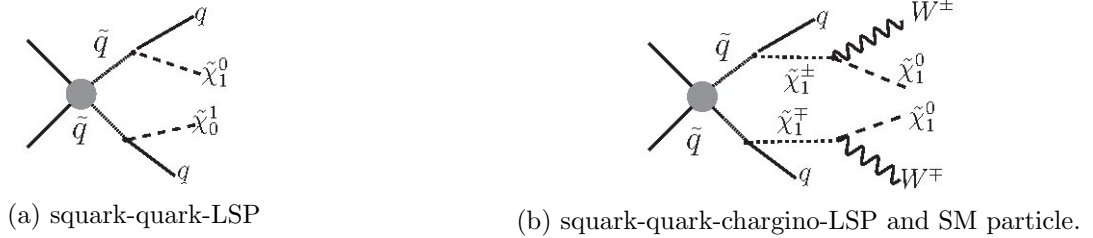


Figure 9: The figure 9a represents a T2 SMS topology. For a sbottom or a stop pair production and decay, they are recognized as T2tt or T2bb. (Implemented in Fastlim and SModelS). The figure 9b is the diagram of the T6WW SMS topology, where it could be a T6WW production (first and second squarks generations) or a T6bbWW (bottom squark production), both for SModelS only.

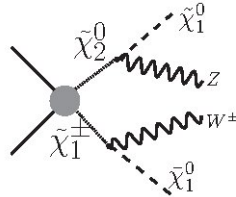


Figure 10: TChiWZ SMS topology, for SModelS.

For the analysis ATLAS_CONF_2013_047, SModelS is implementing the topologies T6WW and T2: the first topology (T6WW) has a $R < 1$, while the second topology (T2) with ($R > 1$) excludes this point.

Fastlim does not consider the T6WW topology, and then it does not exclude the point. This limitation in the topologies implemented is the reason of why one of them is excluding the configuration, while the other is not.

Point 2

This mass spectrum kinetically admits the production of 1st and 2nd squarks generations, the lighter bottom squark mass eigenstate, \tilde{b}_1 , and the lighter top squark mass eigenstate, \tilde{t}_1 . It also allows the production of the two lightest neutralinos, $\tilde{\chi}_{1,2}^0$; the gluino, \tilde{g} , and the lightest chargino, $\tilde{\chi}_1^\pm$.

The masses of the second neutralino, $\tilde{\chi}_2^0$, and the lightest chargino are alike once again: the LSP is a bino like, while $\tilde{\chi}_2^0$ and $\tilde{\chi}_1^+$ are wino like. From the mixing matrix is possible to conclude that the top squark \tilde{t}_1 and the bottom squark \tilde{b}_1 are left-handed dominated.

With this information, it could be expected to have a behaviour similar to the previous file. Some of the decays are forbidden: the mass of \tilde{t}_1 , \tilde{b}_1 , $\tilde{\chi}_2^0$ and $\tilde{\chi}_1^+$ are similar within this mass spectrum. Therefore, the following decays are not allowed: $\tilde{t}_1 \rightarrow t \tilde{\chi}_2^0$ and $\tilde{b}_1 \rightarrow t \tilde{\chi}_1^+$.

Consequently, it is possible to have just the topologies of the following list (and the two first squarks generations production and decays):

$$\begin{array}{lll} \tilde{\chi}_1^\pm \rightarrow \tilde{\chi}_1^0 W^\pm & \tilde{t}_1 \rightarrow \tilde{\chi}_1^0 t & \tilde{b}_1 \rightarrow \tilde{\chi}_1^0 b \\ \tilde{\chi}_2^0 \rightarrow \tilde{\chi}_1^0 Z & \tilde{t}_1 \rightarrow \tilde{\chi}_1^+ b & \tilde{b}_1 \rightarrow \tilde{\chi}_2^0 b \end{array}$$

Possible decays for this mass spectrum

Now then, the topologies implemented by SModelS and Fastlim are shown in the Table 5 (again, the naming convention is described in the Appendix A and these list have no particular order).

SModelS	Fastlim
T2tt (11)	B1bN1_B1bN1 (11)
TChiWZon (12a)	T1tN1_T1tN1 (11)
T6WW (12b)	GtT1tN1_GtT1tN1 (13)
T2 (11)	GbB1bN1_GbB1bN1 (13)
T6bbWW (12b)	
T2bb (11)	

Table 5: Topologies implemented by SModelS and Fastlim (and the number of their respective diagram).

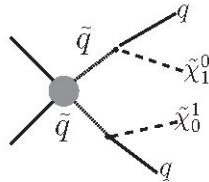


Figure 11: Squark production (squark-quark-LSP). A T2 SMS topology, the squark \tilde{q} could be here a top squark or a bottom squark for both tools (T2tt-T2bb for SModelS and B1bN1-T1tN1 for Fastlim) or just a first or second squarks generations for SModelS.

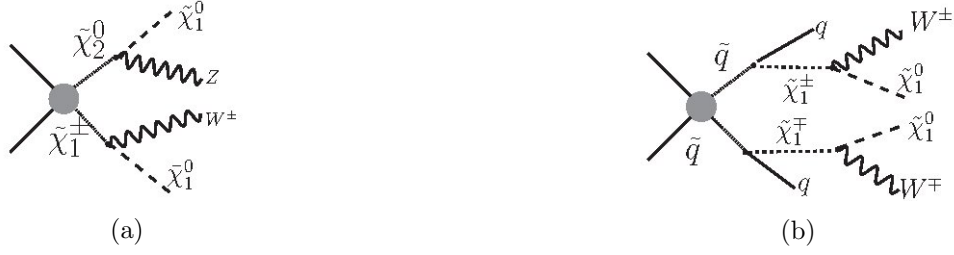


Figure 12: (12a) Chargino-Neutralino production, TChiWZ SMS topology for SModelS. (12b) Squark production, where the squark could be a first or second squark generation or a top squark, T6WW and T6bbWW SMS topologies for SModelS.

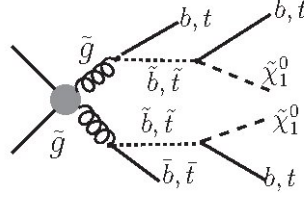


Figure 13: A gluino production, with a top or bottom squark in the decay: GtT1tN1 or GbB1bN1 for Fastlim.

For ATLAS_CONF_2013_047, SModelS excludes the point by a T2 topology, while the point is allowed by Fastlim. Since Fastlim does not consider the production of first two generations squarks it cannot exclude the point but SModelS can.

Point 3

The mass spectrum kinetically allows the production of first and second squarks generations and only the lightest top squark mass eigenstate, \tilde{t}_1 . It also allows the production of the two lightest neutralinos, $\tilde{\chi}_{1,2}^0$; the gluino, \tilde{g} , and the lightest chargino, $\tilde{\chi}_1^\pm$.

The LSP is mainly bino like, while the neutralino $\tilde{\chi}_2^0$ and the chargino $\tilde{\chi}_1^\pm$ have a strong mixing wino-higgsino, still the wino part has a strong presence. The top and bottom squark mixing matrices present a strong a right-handed dominance.

Thus one could expect the following decays:

$$\begin{aligned} \tilde{\chi}_1^\pm &\rightarrow \tilde{\chi}_1^0 W^\pm & \tilde{t}_1 &\rightarrow \tilde{\chi}_1^0 t \\ \tilde{\chi}_2^0 &\rightarrow \tilde{\chi}_1^0 Z \end{aligned}$$

Possible decays for this mass spectrum.

Since the top squark decays to a top plus LSP is kinematically inaccessible, it is more probable to produce $\tilde{t}_1 \rightarrow \tilde{\chi}_1^0 (b W^\pm)$.

The topologies implemented by SModelS and Fastlim are in the Table 6

SModelS	Fastlim
T6WW (15a)	GbB1bN1_GbB1bN1 (15b)
T2 (14)	B1bN1_B1bN1 (14)
T6bbWW (15a)	

Table 6: Topologies implemented by SModelS and Fastlim (and their diagrams).

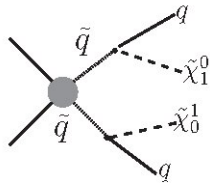


Figure 14: Squark production (squark-quark-LSP), T2 SMS topology. Here, for SModelS the squark (quark) could be first-second squark (quark) generations -T2- or, for Fastlim, a bottom squark (quark) production -B1bN1-.



Figure 15: Squark production, 15a, T6WW or T6bbWW topologies for SModelS. Gluino production, 15b, with bottom squark topology (GbB1bN1) for Fastlim.

When the analysis ATLAS_CONF_2013_047 is confronted with the theoretical prediction, it is founded once again that SModelS is taking into considerations the T6WW and T2 topologies, excluding this mass spectrum configuration, while for Fastlim the sum of all the topologies contribution to the ratio is less than the unit (<1), however the topologies consider by SModelS are different than Fastlim, and that drives to the exclusion of the spectrum.

Brief Summary

So far, these first results explain the behaviour of the tools when analysing the parameter space and comparing their results. The addition of topologies for Fastlim, the consideration of Natural SUSY topologies for Fastlim, and the input parameters of control defined by the user for SModelS, they seem to be playing a role in the exclusion of the mass spectrum. More examples were done for generic spectrum decomposition with Fastlim and SModelS, they are in Appendix C.

5 Natural Supersymmetry SMS interpretation

5.1 Setup of the study

To illustrate the employment of SModels and Fastlim, it is more useful to re-interpret a model of interest. For this purpose, it was studied the natural SUSY scenario, a well known region of the SUSY parameter space, which provides a simple mass spectrum and topologies, to make a comparison between the two framework results.

A total number of 2045 points were taken:

- One light top squark eigenstate within a range 150 GeV up to 750 GeV; a left-handed sbottom, when the $\theta_t = 0$. Three stop mixing angles were considered, $\theta_t = 0, \pi/4$ and $\pi/2$.
- the μ term (Higgsino mass) is in the range 100 GeV up to 750 GeV
- the gluino is 2000 GeV

- the Yukawa coupling depends on the value of β angle, then two extreme cases were considered: $\tan[\beta] = 10$ or 50 , at the m_Z value
- all the other SUSY particles were heavy.

As this spectrum, described before for natural SUSY (Section 1.3), has the property that all the electro-weakino particles are quasi-degenerated (their masses are more or less the same), therefore, the decay of the heavier neutralino $\tilde{\chi}_2^0$ and $\tilde{\chi}_1^\pm$ are unobservable: the final states will be $tt + \text{MET}$ or $bb + \text{MET}$, that are coming whether from a top squark decay or bottom squark decay.

Then, the possible decay chains are the following:

$$\begin{array}{lll} \tilde{t}_{1,2} \rightarrow \tilde{\chi}_1^0 t & \tilde{b}_1 \rightarrow \tilde{\chi}_1^0 b & \tilde{g} \rightarrow b \bar{b} \tilde{\chi}_1^0 \\ \tilde{t}_{1,2} \rightarrow \tilde{\chi}_2^0 t & \tilde{b}_1 \rightarrow \tilde{\chi}_2^0 b & \tilde{g} \rightarrow t \bar{t} \tilde{\chi}_1^0 \\ \tilde{t}_{1,2} \rightarrow \tilde{\chi}_1^\pm t & \tilde{b}_1 \rightarrow \tilde{\chi}_1^\pm b & \end{array}$$

Possible decays for the mass spectrum.

5.2 Constraining the parameter space: excluded points from the mass spectrum

The excluded points for each tool were marginalized for θ_t , to obtain them independently of the mixing angle for the top squark mass matrix. The procedure was to look for the common excluded points in the mass spectrum for both tools in first place, and secondly to consider only the common experimental analyses implemented for both tools. That will allow us to interpret the exclusion area from SModelS and Fastlim.

The study was divided in two parts: a small $\tan[\beta]$ value and the extreme case a large $\tan[\beta]$ value.

5.2.1 $\tan[\beta] = 10$

For a small $\tan[\beta]$, the Figure 16 and Figure 24 (Appendix D) are showing the exclusion area for the bottom squark and the top squark, respectively.

The observed exclusion area in the plot from Figure 16 for a neutralino up 200 GeV, with a bottom squark in a range from 150 GeV up to ~ 375 GeV, it is covered broadly by common excluded points from Fastlim and SModelS, giving an almost homogeneous excluded sector of points in the mass spectrum. However, around 400 GeV and beyond (up to 500 GeV), for the same neutralino mass, Fastlim is excluding some more bottom squark mass values. While, SModelS adds almost a whole line of excluded points for a larger value of LSP, above 240 GeV.

To have a better understanding about the nature of these excluded points, the plot with only the common analyses is necessary. There, it is possible to observe that not only the extra excluded points from SModelS are coming from the non-common analyses between the two, but also thanks to those extra analyses implemented SModelS has a description of the exclusion area as good as Fastlim. The Fastlim extra excluded points, in other hand, are coming from common analyses. Why is it Fastlim having an exclusion and SModelS is not within that range? After interpreting the results obtained, the best explanation falls over the efficiency maps and the ability of adding topologies from Fastlim. For instance, when looking into some of these results, it used to happen that only a few topologies were actually excluded as individual topology (with a value of R larger than the unity). Instead, the value $R > 1$ for the exclusion ratio was a result of the sum of individual exclusion ratios from each possible topology in that point, as it is stated in the example from Table 7.

The analysis is similar for the top squark exclusion area, for these mass spectrum configuration (Figure 24). The exclusion area from the common points from Fastlim and SModelS, it is set for a top squark mass between 200 GeV and 400 GeV, for a neutralino LSP up to 200 GeV.

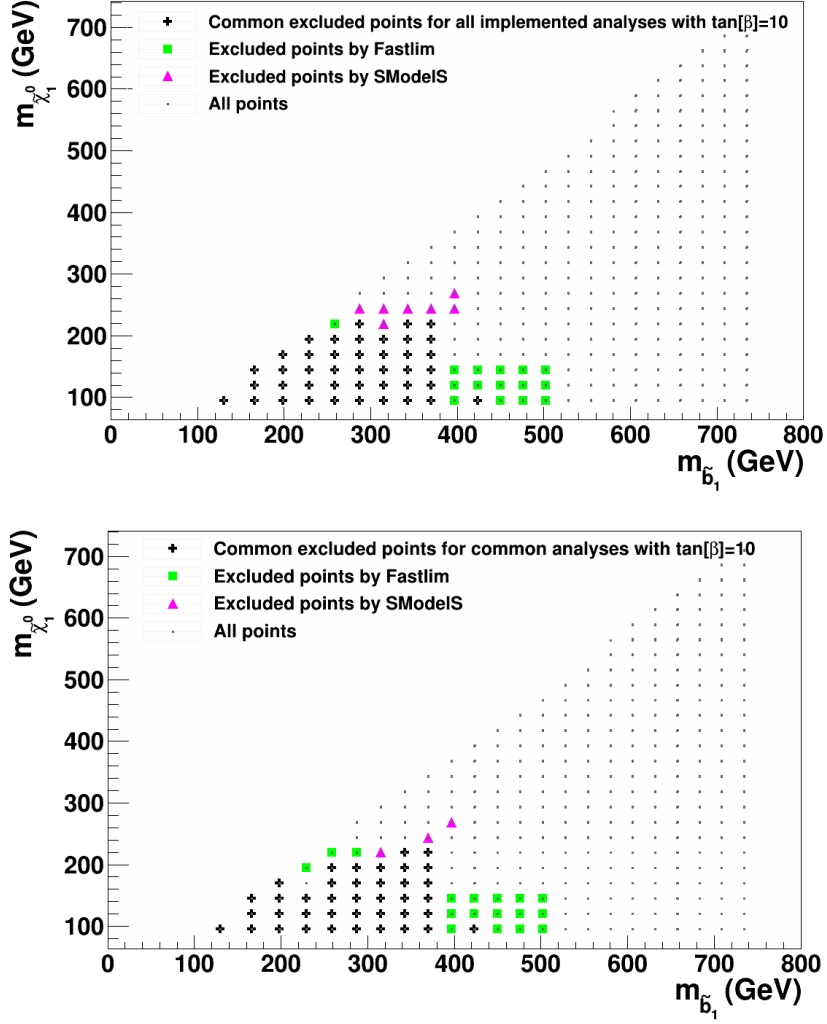


Figure 16: Left-handed bottom squark - LSP marginalized exclusion plot for $\tan\beta = 10$. The black points show the common excluded points between SModelS and Fastlim, the pink points show those excluded by SModelS but not by Fastlim, and vice versa the green points. The up-plot corresponds to all the implemented analyses by both tools, while the down-plot shows only the common analyses implemented.

ATLAS_CONF_2013_024	
SModelS	Fastlim
R = 0.6	R = 1.16
T2tt, R=0.6	T1tN1_T1tN1 r=0.61 B1bN1_B1bN1 r=0.0002 T1bN1_T1bN1 r=0.0637 B1tN1_B1tN1 r=0.0042 T1bN1_T1tN1 r=0.4798 B1tN1_B1bN1 r=0.0018

Table 7: Topologies implemented by SModelS and Fastlim, to exclude certain $m_{\tilde{\chi}_1^0} \sim 119$ GeV and $m_{\tilde{b}_1} \sim 397$ GeV from the mass spectrum. This topology decomposition and result for $\theta_t = \pi/4$

If it is studied case by case each of the top squark mixing angle used to marginalize the previous plot

(for instance, for a fixed $\tan[\beta] = 10$), it is possible to remark differences in the exclusion methodology of the tools, due the chosen spectrum configuration.

For $\theta_t = 0$, left-, right-handed stop mixing is neglected. It will exist the presence of a left-handed sbottom and a bit heavier left-handed stop. Due the presence of the sbottom, more limits are set and more excluded points are observed in the results from both tools, it could be said that almost double the number of points excluded for any of the other angles. In the plots from Figure 25 (Appendix D), the excluded points are for $m_{\tilde{t}_1}$ in a range equal to 200-725 GeV, mostly for a neutralino LSP below 200 GeV. The exclusion area is enlarge up to 750 GeV for SModelS. When the common analyses plot is compared with the result from the implementation of all the analyses. It is possible to notice that the extra set of analyses implemented by SModelS, makes an exclusion of points comparable with those obtained from the efficiency maps from Fastlim.

For $\theta_t = 90$, left-, right-handed stop mixing is also neglected. In this case, it will be only a right top squark. For the common excluded points (plots in Figure 26, in Appendix D), an homogeneous exclusion area lives in a range between 200 GeV and 450 GeV for the stop mass, with a neutralino LSP below 200 GeV. SModelS is able to excluded a sector for small values of stop and neutralino mass (150 GeV - 200 GeV, for a neutralino lighter than 150 GeV) and also to include a new line of exclude points around 250 GeV, while Fastlim is able to add excluded points for heavier stops. In general, Fastlim will exclude in a better way points for heavier stops and light neutralinos, instead of describing heavier neutralinos, due the efficiency maps: they are less accurate as the neutralino mass is getting heavier. This last statement is valid for all the mixing angle θ_t .

For $\theta_t = 45$ is not so trivial, because it has left- and right-handed stop mixing. The area of excluded points is going to be smaller than for the previous angles, for those common ones (see plots in Figure 27 in the Appendix D). SModelS takes the consideration that there is a dominant topology, thus it is hard to read the excluded points, because the signals are not going to be strong enough to exclude one or the other. That means, it will have less excluded points than Fastlim, that is able to add the contributions from all the possible topologies and this sum will generally exclude the point. As it was expected, the excluded area due Fastlim is larger and it includes heavy stops (up to 550 GeV) for light neutralinos (150 GeV and below).

5.2.2 $\tan[\beta] = 50$

The re-interpretation for $\tan[\beta]=50$ is shown for top squark plot in Figure 17 and for bottom squark plot in Figure 28 (Appendix D). The exclusion area for a neutralino LSP up to 200 GeV and top squark mass value between 200 GeV and 400 GeV, show the common points between the results obtained by Fastlim and SModelS. Once again, the extra points obtained for each tool seem to be located in very specific places: a line of excluded points for a heavier LSP value (250 GeV) obtained by SModelS, and heavier top squark mass points are excluded for a LSP with mass value below 200 GeV by Fastlim.

But, within a marginalized consideration of θ_t , the exclusion areas are identical for common and non-common analyses.

The $\tan[\beta]$ tells information about the Yukawa couplings and the dominant topologies. In general, this will affect the shape of the exclusion areas. When $\tan[\beta]$ is small, the dominant topology will be T2tt, while the dominant topology for a large $\tan[\beta]$ will have T2bb topology as dominant.

The last statement has importance, for example, in the points excluded by Fastlim due the dominant topologies in the used limits. This is involved with the shape description of excluded area of Fastlim.

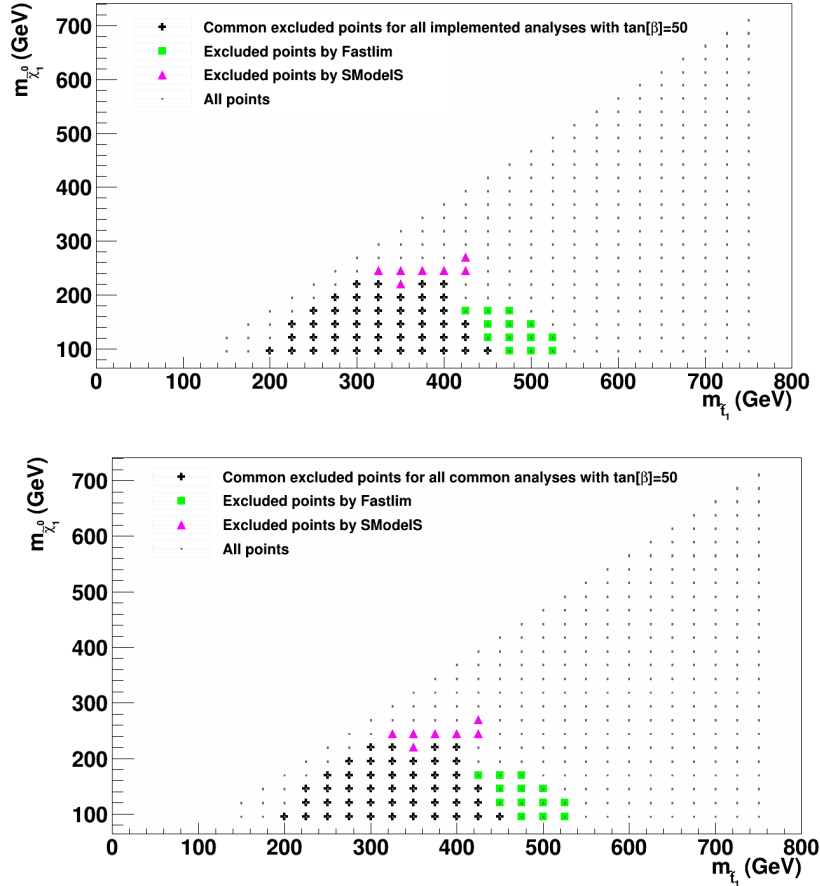


Figure 17: Top squark - LSP marginalized exclusion plot for $\tan\beta = 50$. The black points show the common excluded points between SModelS and Fastlim, the pink points show those excluded by SModelS but not by Fastlim, and vice versa the green points. The up-plot corresponds to all the implemented analyses by both tools, while the down-plot shows only the common analyses implemented.

6 Conclusions

The purpose of this work was to understand the SMS approach, by decomposing SUSY scenarios and using two automated tools, to obtain a re-interpretation of the parameter space.

A generic interpretation, that allows to constraint as many models as possible, is useful. This will enable to keep valid a theoretical prediction in terms of the experimental results that are available so far. Because of that, the SMS offers an important phenomenological approach, able to re-interpret the experimental results independently of the (SUSY) model.

The philosophy of SMS aim to involve a small number of parameters and particles; having as main idea that any model can be decompose in terms of SMS topologies. These statements were confirmed in the first part of this work, where some points of arbitrary SUSY models were interpreted within the SMS approach.

To achieve the interpretation and constrain the SUSY parameter space for these points, two automated tools were used: SModelS and Fastlim. Both tools decompose the spectrum into SMS topologies, then they confront the theoretical predictions against the experimental limits. However, they have different methodologies, and differences appear in the results.

From that first part, one can conclude that, the different topologies implemented by each of the tools has consequences in the excluded points. For instance, SModelS decomposed the spectrum in different topologies that were not considered by Fastlim, and that let it excluded different points in those examples.

After understanding the role that topologies play in the exclusion of the points, a model of interest was studied, with a total of 2045 points: a natural SUSY model, which was re-interpreted within the SMS approach, and decomposed using SModelS and Fastlim.

From the comparison of their results, it is possible to conclude that: SModelS has a more generic decomposition and a larger number of analyses implemented than Fastlim. Fastlim has the property to add the different topologies, thanks to the efficiency maps, and this is fundamental when it is not present a dominant topology. However, they have nearly the same exclusion area.

The main difference between SModelS and Fastlim resides in the decomposition and exclusion methodology: the efficiency maps vs. a single dominant topology. Sometimes a single topology is not enough to exclude a point in the mass spectrum, and it is the addition of the contributions of all the possible topologies who excludes the point. However, the efficiency maps are also limited: they are not able to have a precise exclusion for heavy neutralino mass values.

In the other hand, generic topologies are also useful to have a complete description of the parameter space and the excluded points. While, one topology is allowing certain mass configuration, it might happen that another one excludes it. Then, Fastlim is limited due to the use of natural SUSY topologies only.

It is important to emphasize that the main objective of this work, the decomposition of a SUSY model within the SMS approach, was achieved. But, it is also important to recall that the decomposition of the spectrum, using the automated tools is not perfect, more SMS topologies are needed to have a more general interpretation.

A Nomenclature

This work uses the SMS conventions of the CMS collaboration [16]. The following is a short guideline of the topologies names (and topologies list) implemented by each tool and in this work.

Work naming convention:

- T1 model: the simplified version of gluino pair production and three-body decay into light-flavor quark-antiquark and the LSP.
- T2 model: the simplified version of squark-antisquark production, where each squark undergoes a two body decay to a light-flavor quark and the LSP.
- T3 model: the simplified version of gluino pair production, but this time one of the gluinos decay as in T1 model, while the other one has a cascade decay through an intermediate particle ($\tilde{\chi}_2^0$ or $\tilde{\chi}_1^\pm$).
- T5 model: another gluino pair production, but both gluinos undergo cascade decays. It could go to a three-body decay to a lepton-neutrino-LSP, a two-body decay to a Z boson-LSP or the quark-antiquark pair and an intermediate neutralino, which decays to a photon and a massless LSP.
- T6 model: a similar simplified version of the squark-antisquark production, but that will produce at the end a W boson and the LSP (plus the corresponding quark).
- TChi models: the simplified versions of the direct production and decay of charginos and neutralinos, or neutralinos pairs.

Model		Production	Decay
T1	simplified version of a gluino par production.	$\tilde{g}\tilde{g}$	$\tilde{g} \rightarrow q \bar{q}\tilde{\chi}_{LSP}$
T1bbbb	gluino pair production, decays into b pair.	$\tilde{g}\tilde{g}$	$\tilde{g} \rightarrow b \bar{b}\tilde{\chi}_{LSP}$
T1tttt	gluino pair production, decays into t pair.	$\tilde{g}\tilde{g}$	$\tilde{g} \rightarrow t \bar{t}\tilde{\chi}_{LSP}$
T2	simplified version of squark-antisquark.	$\tilde{q}\tilde{q}^*$	$\tilde{q} \rightarrow q \tilde{\chi}_{LSP}$
T2bb	bottom squark production.	$\tilde{b}\tilde{b}^*$	$\tilde{b} \rightarrow b \tilde{\chi}_{LSP}$
T2tt	top squark production.	$\tilde{t}\tilde{t}^*$	$\tilde{t} \rightarrow t \tilde{\chi}_{LSP}$
T6ttww	direct bottom squark production, it decays to a top quark, a W boson and the LSP.	$\tilde{b}\tilde{b}^*$	$\tilde{b} \rightarrow t \tilde{\chi}^-$, $\tilde{\chi}^- \rightarrow W^- \tilde{\chi}_{LSP}$
T6bbww	direct top squark production: it decays to a bottom quark, a W boson and the LSP.	$\tilde{t}\tilde{t}^*$	$\tilde{t} \rightarrow b \tilde{\chi}^-$, $\tilde{\chi}^- \rightarrow W^- \tilde{\chi}_{LSP}$
TChiSlepSlep	simplified version of direct chargino-neutralino production.	$\tilde{\chi}_1^\pm \tilde{\chi}_2^0$	$\tilde{\chi}_2^0 \rightarrow l^{pm} \tilde{l}^\mp$, $\tilde{l} \rightarrow l \tilde{\chi}_{LSP}$ $\tilde{\chi}_1^\pm \rightarrow \nu \tilde{l}^{pm}$, $\tilde{l}^\pm \rightarrow l^\pm \tilde{\chi}_{LSP}$
TChiwz	simplified version of direct chargino-neutralino production	$\tilde{\chi}_1^\pm \tilde{\chi}_2^0$	$\tilde{\chi}_2^0 \rightarrow Z \tilde{\chi}_{LSP}$, $\tilde{\chi}_1^\pm \rightarrow W^\pm \tilde{\chi}_{LSP}$

Table 8: SModelS Nomenclature: SMS possible topologies and names [16].

In addition, the nomenclature of the particles (and sparticles) used by Fastlim is in the Table 9. Yet the tool uses only natural SUSY topologies, so only certain topologies will be present.

SM Particle Name	g	γ	Z	h	H	A	W^\pm	H^\pm			
	g	gam	z	h	h2	h3	w	hp			
SUSY Particle Name	\tilde{g}	$\tilde{\chi}_1^0$	$\tilde{\chi}_2^0$	$\tilde{\chi}_3^0$	$\tilde{\chi}_4^0$		$\tilde{\chi}_1^\pm$	$\tilde{\chi}_2^\pm$			
	G	N1	N2	N3	N4		C1	C2			
SM Particle Name	q	t	b	e	μ	τ		ν			
	q	t	b	e	m	ta		n			
SUSY Particle Name	\tilde{q}	\tilde{t}_1	\tilde{t}_2	\tilde{b}_1	\tilde{b}_2	\tilde{e}	$\tilde{\mu}$	$\tilde{\tau}_1$	$\tilde{\tau}_2$	$\tilde{\nu}$	$\tilde{\nu}_\tau$
	Q	T1	T2	B1	B2	E	M	TAU1	TAU2	NU	NUT

Table 9: Fastlim nomenclature: particles and sparticles names [12].

B List of SUSY Analyses implemented

It is useful to look into the analyses in database implemented by Fastlim and SModelS: when this work was done, Fastlim had eleven analyses available while SModelS had more than forty implemented analyses (yet this number is increasing). Actually, both tools are using some common analyses for the SMS interpretation. Then, it results interesting to observe the behaviour of both tools with either all the set of analyses or only the common ones, to make a comparison between their performance.

- Common analyses implemented by SModelS and Fastlim:

Squark third generation production (bottom-top squarks) analyses:

ATLAS_CONF_2013.024 [11]; ATLAS_CONF_2013.037 [17]; ATLAS_CONF_2013.053 [18]; ATLAS_CONF_2013.048 [19].

Electroweakino production (charginos-neutralinos) analyses:

ATLAS_CONF_2013.035 [20]; ATLAS_CONF_2013.093 [21].

Third generation squark + hadronic (gluino and first squarks generations) production analyses:

ATLAS_CONF_2013.047 [15]; ATLAS_CONF_2013.061 [22].

Direct sleptons production analyses:

ATLAS_CONF_2013.049 [23].

- Analyses implemented only by SModelS:

ATLAS:

(hadronic production) ATLAS_CONF_2013.007 [24], SUSY_2013.04 [25], ATLAS_CONF_2012.105 [26], ATLAS_CONF_2013.089 [27], ATLAS_CONF_2013.062 [28]; **(squark third generation production)** ATLAS_CONF_2013.025 [29]; ATLAS_CONF_2012.166 [30]; ATLAS_CONF_2013.001 [31]; ATLAS_CONF_2013.007 [24]; SUSY_2013.05 [32]; ATLAS_CONF_2013.065 [33]; **(electroweakino production)** ATLAS_CONF_2013.036 [34]; ATLAS_CONF_2013.028 [35].

CMS:

(hadronic production) SUS-12-026 [36]; SUS-13-008 [37]; SUS-13-004 [38]; SUS-12-024 [39]; SUS-13-016 [40]; SUS-12-028 [41]; SUS-13-012 [42]; SUS-13-013 [43]; SUS-13-002 [44]; SUS-13-007 [45]; **(squark third generation production)** SUS-13-008 [37]; SUS-13-013 [43]; SUS-12-024 [39]; SUS-12-028 [41]; SUS-13-011 [46]; SUS-13-004 [38]; SUS-13-002 [44]; **(Electroweakino + direct sleptons production)** SUS-12-022 [47]; SUS-13-006 [48]; SUS-13-001 [49].

- Analyses implemented only by Fastlim:

(**squark third generation + hadronic production**) ATLAS_CONF_2013_054 [50].

It is convenient to take the common analyses for both tools and to examine the topologies decomposition for the same files. That would make more clear the subtle differences in the decomposition implemented by each of the tool and the consequences in the re-interpretation of the experimental results. Consequently, from the common set, the analyses ATLAS_CONF_2013_024 and ATLAS_CONF_2013_037 were taken and their information from Fastlim and SModelS were compared.

ATLAS_CONF_2013_024: *Search for direct production of the top squark in the all-hadronic $t\bar{t} + E_T^{miss}$ final state in 21 fb^{-1} of pp collisions at $\sqrt{s} = 8 \text{ TeV}$ with the ATLAS detector [11].*

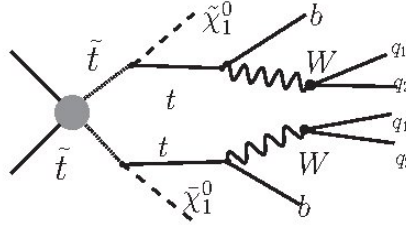


Figure 18: The particle production considered in the analysis ATLAS_CONF_2013_024 [11].

The dominant topology chose experimentally is a top squark decaying to a top quark and the lightest SUSY Particle (LSP), in a RPC scenario (just as shown in the Figure 18). This search is conducted in events with large missing transverse momentum and six or more jets.

Now, the SMS topologies considered for the re-interpretation by the tools are the following:

- SModelS topology: a single topology considered, T2tt or, in other words, a simplified top squark-antisquark production; the top squark could be any of the mass mixing \tilde{t}_1 or \tilde{t}_2 , decaying into a top quark and the LSP (Figure 19).

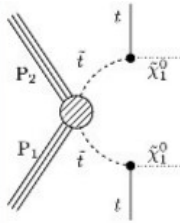


Figure 19: SModelS topology for ATLAS_CONF_2013_024 analysis, figure taken from [9].

- Fastlim topology: The main contributing topologies considered in the efficiency tables are T1bN1_T1bN1, T1bN1_T1tN1 and T1tN1_T1tN1 (Figure 20), or a top squark-antisquark decaying into top quark and the LSP. However, due to the considerations in the topologies taken by Fastlim (natural SUSY), it could also go to a bottom quark and the LSP (as explained in 1.3).

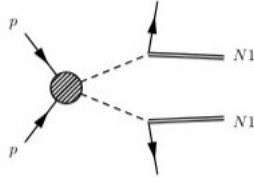


Figure 20: Fastlim topology for ATLAS_CONF_2013-024 analysis, figure taken from [12].

ATLAS_CONF_2013_037: Search for direct top squark pair production in final states with one isolated lepton, jets and missing transverse momentum in $\sqrt{s} = 8 \text{ TeV}$ pp collisions [17].

The experimental search is for a direct top squark pair production and a final state with one isolated lepton (electron or muon) and MET. Experimentally, the dominant topology is a top squark decaying into SM quarks and $\tilde{\chi}_1^\pm$.

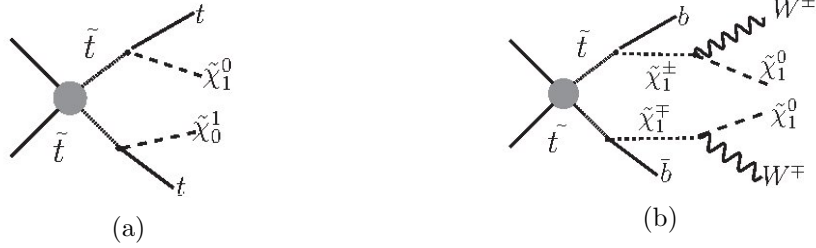


Figure 21: Diagrams of the particle production considered in the analysis ATLAS_CONF_2013-037 [17].

Then, the final state could be characterised by a top-antitop quark pair produced together with possible large MET, $\tilde{t}_1 \rightarrow t + \tilde{\chi}_1^0$ (Figure 21a); or two W bosons, two jets originated from b-quarks (b-jets) and MET with different kinematic properties with respect to the first one, $\tilde{t}_1 \rightarrow b + \tilde{\chi}_1^\pm \setminus \tilde{\chi}_1^\pm \rightarrow W^\pm + \tilde{\chi}_1^0$. Figure 21b shows both productions.

The SMS decomposition by SModelS and Fastlim is:

- SModelS topology: the signal of the spectrum is decomposed into two SMS topologies; a T2tt topology, or simplified top squark-antisquark production as the one in Figure 22a, and a T6bbww topology, or direct production of a top squark that decays to a bottom quark-W boson-LSP, as shown in Figure 22b.

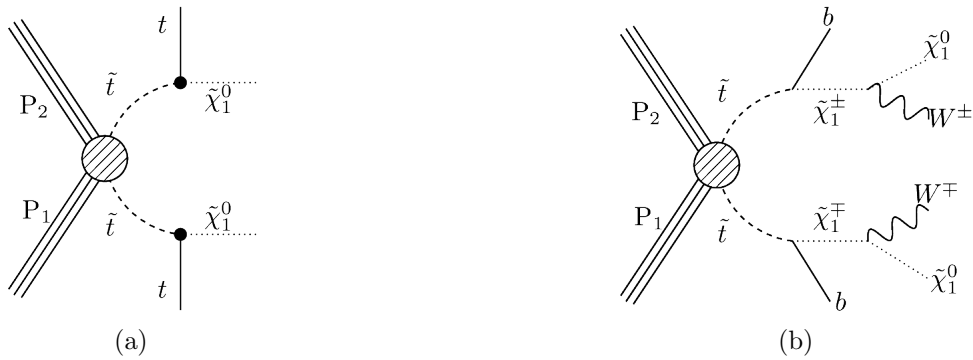


Figure 22: SModelS topologies for ATLAS_CONF_2013.037, figure taken from [9].

- Fastlim topology: The contributing topologies for Fastlim are once again T1bN1_T1bN1, T1bN1_T1tN1 and T1tN1_T1tN1 (shown in Figure 23).

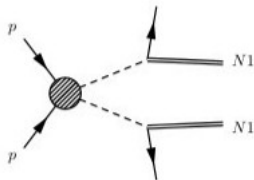


Figure 23: Fastlim topologies for ATLAS_CONF_2013_037, taken from [12].

C SMS decomposition examples

This part is also a comparison between the decomposition of arbitrary SUSY spectra, using Fastlim and SModelS tools. This time, nine files with different mass spectrum configuration were taken and interpreted by Fastlim and SModelS. Once again, it is presented a table with the experimental analyses implemented and if the configuration is excluded or not when confronted the experimental bounds and the theoretical predictions (Table 10).

The points 1 and 9 are excluding the configuration when the spectrum configuration is analysed with SModelS and not with Fastlim, but once again it is due to the different signal topologies combination done by both (SModelS is considering a T6bbWW topology, while SModelS is considering T2tt and T2bb topologies).

The novel here are for the points 2, 4 and 7. SModelS is excluding the spectrum configuration when considering the T2tt topology; however, Fastlim is not, despite it considers the same topology (T2tt) in their interpretation (Table 11).

Except for the point 7, it would be hard to say that the differences between the ratios are cause by statistics in the production of the events.

With respect to the point 5, the analysis could not be done because a limitation in the Fastlim code at this moment: Fastlim considers that the decay chain is over when the $\tilde{\chi}_{LSP}$ is founded, that means all the decays would have in their final state a $\tilde{\chi}_1^0$ particle. However, the mass spectrum configuration for this point stated that the mass of one of the sparticles (the bottom squark, \tilde{b}_1) is practically the same as the mass of the LSP. This has as implication that the sparticle is also considered as a stable (it does not decay) and that Fastlim does not know how to interpret it, leading to code errors.

The point 3, the point 8 and the point 6 show coherence between the results for Fastlim and SModelS: at the point 3 and 8 the configuration in not excluded by any of the tools when the theoretical expectations and the experimental bounds are confronted. While, at the point 6 both are excluding the configuration with the same SMS topology, T2bb.

	SModelS exclusion ratio	Fastlim exclusion ratio
Point 1	light $\tilde{\chi}_{1,2}^0, \tilde{\chi}_1^\pm, \tilde{t}_1, \tilde{g}$	
ATLAS_CONF_2013_024	<1	<1
ATLAS_CONF_2013_035	<1	<1
ATLAS_CONF_2013_037	<1	<1
⋮	⋮	⋮

\vdots	\vdots	\vdots
ATLAS_CONF_2013_053	<1	<1
ATLAS_CONF_2013_048	>1 Excluded!	<1
topologies	T6bbWW	T1tN1, B1bN1, B2bN1
Point 2 light $\tilde{\chi}_{1,2}^0, \tilde{\chi}_1^\pm, \tilde{t}_1, \tilde{b}_{1,2}, \tilde{g}$		
ATLAS_CONF_2013_024	<1	<1
ATLAS_CONF_2013_035	<1	<1
ATLAS_CONF_2013_037	>1 Excluded!	<1
topologies	T2tt	T1tN1, GtT1tN1
Point 3 light $\tilde{\chi}_{1,2}^0, \tilde{\chi}_1^\pm, \tilde{t}_1, \tilde{b}_{1,2}, \tilde{g}$		
ATLAS_CONF_2013_035	<1	<1
ATLAS_CONF_2013_024	<1	<1
ATLAS_CONF_2013_037	<1	<1
Point 4 light $\tilde{\chi}_{1,2}^0, \tilde{\chi}_1^\pm, \tilde{t}_1, \tilde{b}_{1,2}, \tilde{g}$		
ATLAS_CONF_2013_035	<1	<1
ATLAS_CONF_2013_024	<1	<1
ATLAS_CONF_2013_037	>1 Excluded!	<1
topologies	T2tt	T1tN1, GtT1tN1
Point 5 light $\tilde{\chi}_{1,2}^0, \tilde{\chi}_1^\pm, \tilde{t}_1, \tilde{g}$ It was not possible to do the Fastlim re-interpretation*.		
Point 6 light $\tilde{\chi}_{1,2}^0, \tilde{\chi}_1^\pm, \tilde{t}_1, \tilde{b}_{1,2}, \tilde{g}$		
ATLAS_CONF_2013_048	<1	<1
ATLAS_CONF_2013_053	>1 Excluded!	>1 Excluded!
topologies	T2bb	B1bN1
Point 7 light $\tilde{\chi}_{1,2}^0, \tilde{\chi}_1^\pm, \tilde{t}_{1,2}, \tilde{b}_{1,2}, \tilde{g}$		
ATLAS_CONF_2013_024	<1	<1
ATLAS_CONF_2013_035	<1	<1
ATLAS_CONF_2013_048	<1	<1
ATLAS_CONF_2013_037	>1 Excluded!	<1
topologies	T2tt	T1tN1, T2tN1, GtT1tN1 GtT1tN1_GtT2tN1
Point 8 light $\tilde{\chi}_{1,2,3,4}^0, \tilde{\chi}_{1,2}^\pm, \tilde{t}_1, \tilde{b}_{1,2}, \tilde{g}$		
ATLAS_CONF_2013_024	<1	<1
ATLAS_CONF_2013_037	<1	<1
ATLAS_CONF_2013_047	<1	<1
ATLAS_CONF_2013_062	<1	<1
ATLAS_CONF_2013_053	<1	<1
Point 9 light $\tilde{\chi}_{1,2}^0, \tilde{\chi}_1^\pm, \tilde{t}_1, \tilde{b}_{1,2}, \tilde{g}$		
ATLAS_CONF_2013_024	<1	<1
ATLAS_CONF_2013_035	<1	<1
ATLAS_CONF_2013_037	<1	<1
ATLAS_CONF_2013_053	<1	<1
ATLAS_CONF_2013_048	>1 Excluded!	<1
topologies	T6bbWW	B2bN1, B1bN1, T1tN1

Table 10: Analyses implemented by Fastlim and SModels and their exclusion ratio. * See in the discussion of results.

Analysis	SModelS ratio	Fastlim ratio
Point 2		
ATLAS_CONF_2013_037	R = 1.287E00	R < 0.65
Point 4		
ATLAS_CONF_2013_037	R = 1.249E00	R < 0.65
Point 7		
ATLAS_CONF_2013_037	R = 1.140E00	R < 0.88

Table 11: SModelS and Fastlim exclusion ratio values for the same topologies

D Auxiliary Plots

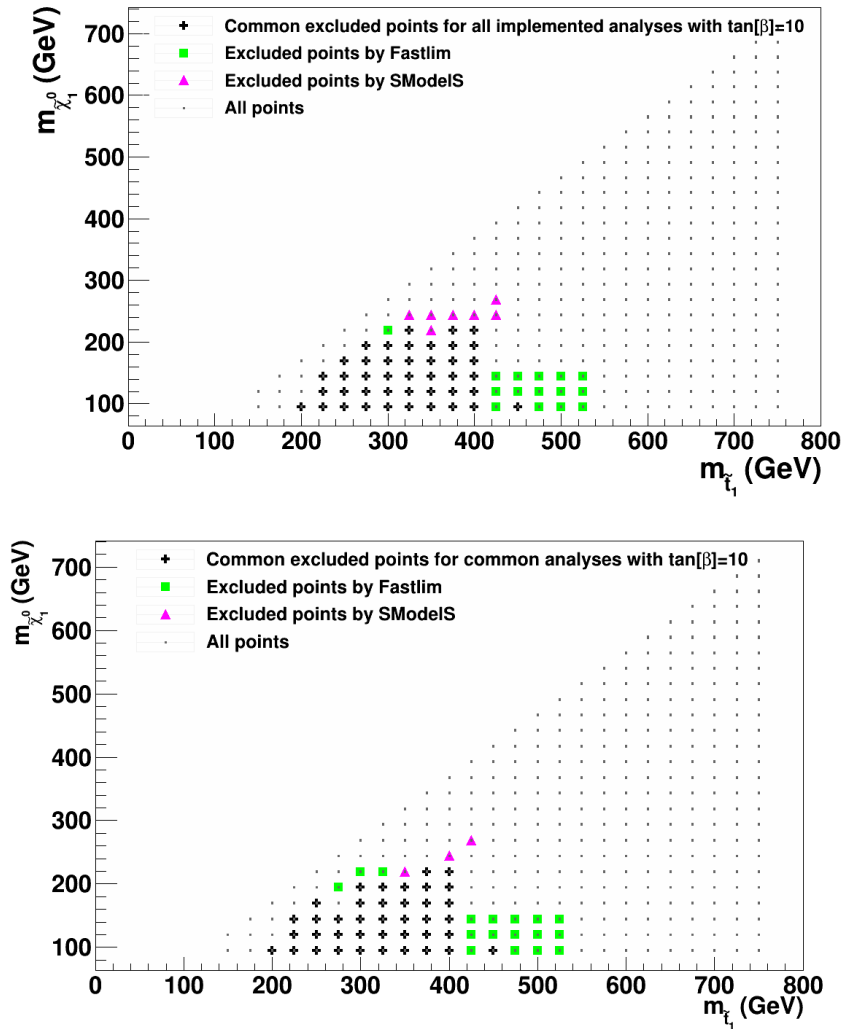


Figure 24: Top squark - LSP marginalized exclusion plot for $\tan\beta = 10$. The black points show the common excluded points between SModelS and Fastlim, the pink points show those excluded by SModelS but not by Fastlim, and vice versa the green points. The up-plot corresponds to all the implemented analyses by both tools, while the down-plot shows only the common analyses implemented.

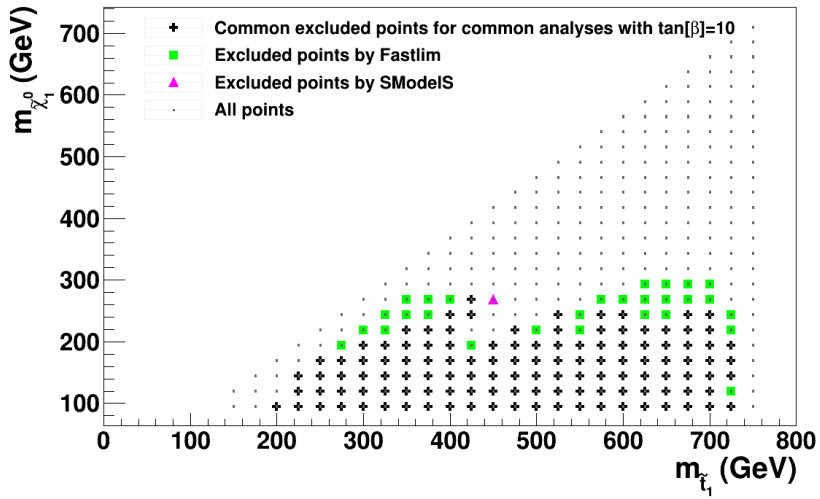
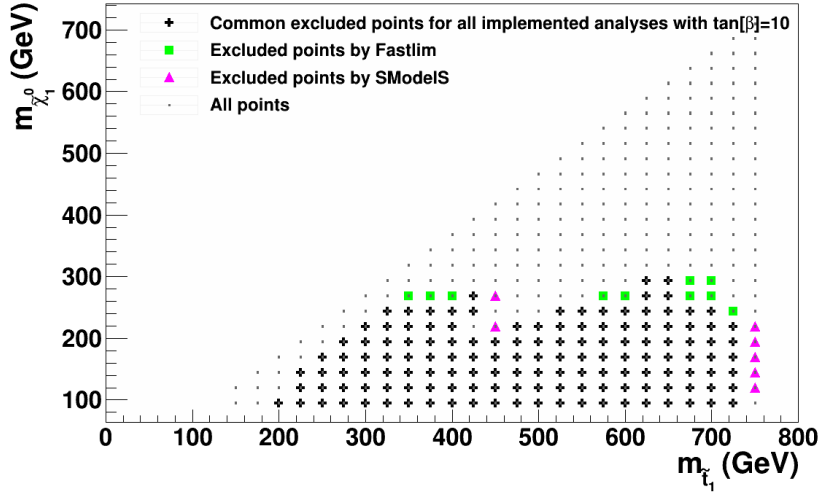


Figure 25: Top squark - LSP exclusion plot for $\tan\beta = 10$ and mixing angle $\theta_t=0$. The black points show the common excluded points between SModelS and Fastlim, the pink points show those excluded by SModelS but not by Fastlim, and vice versa the green points. The up-plot corresponds to all the implemented analyses by both tools, while the down-plot shows only the common analyses implemented.

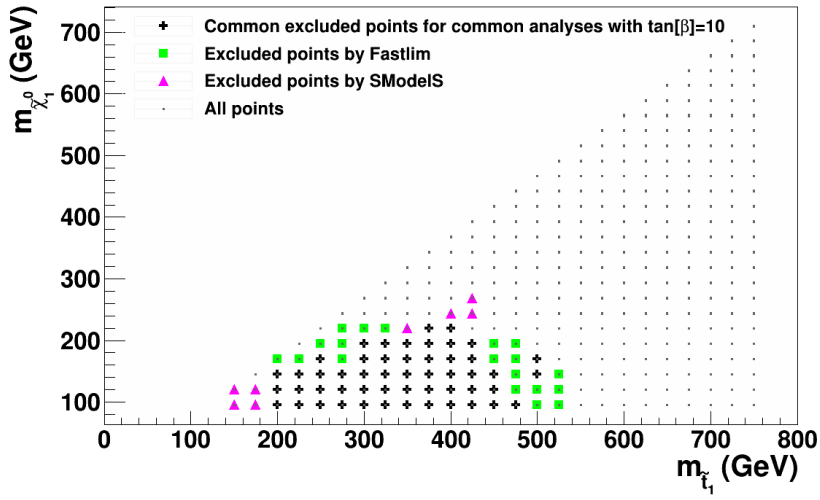
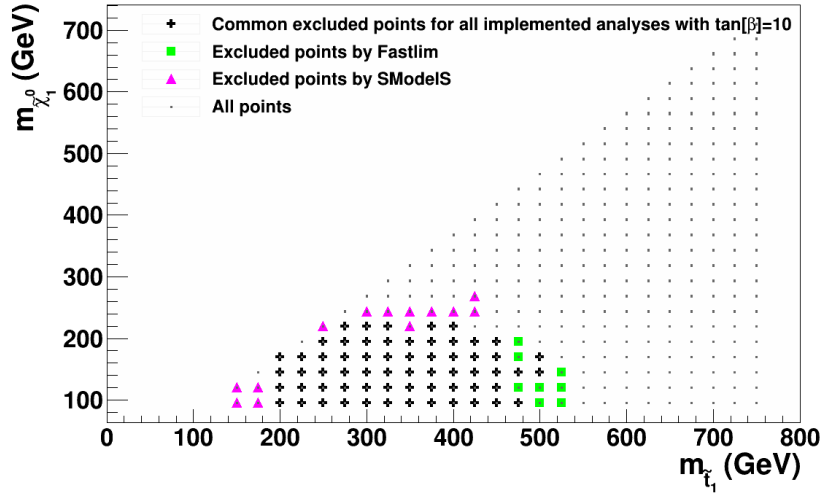


Figure 26: Top squark - LSP exclusion plot for $\tan\beta = 10$ and mixing angle $\theta_t=90$. The black points show the common excluded points between SModelS and Fastlim, the pink points show those excluded by SModelS but not by Fastlim, and vice versa the green points. The up-plot corresponds to all the implemented analyses by both tools, while the down-plot shows only the common analyses implemented.

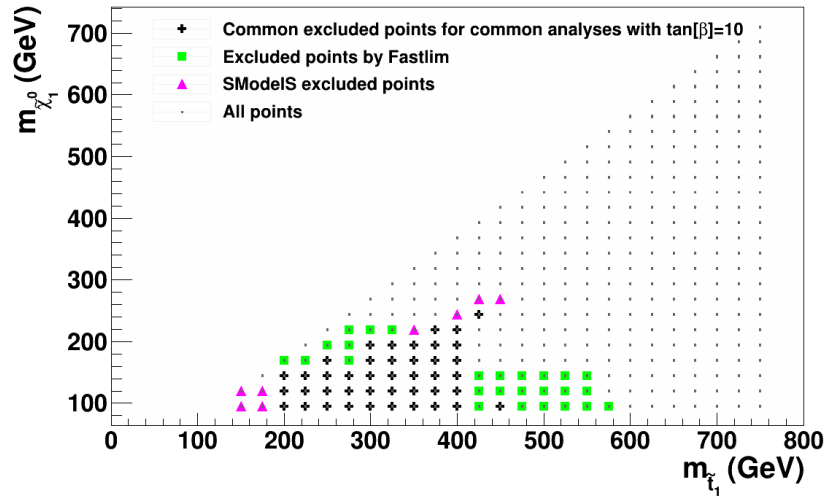
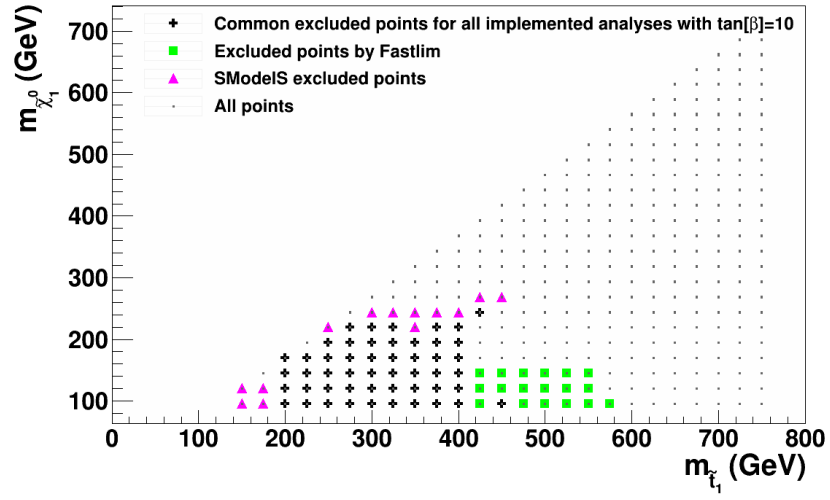


Figure 27: Top squark - LSP exclusion plot for $\tan\beta = 10$ and mixing angle $\theta_t=45$. The black points show the common excluded points between SModelS and Fastlim, the pink points show those excluded by SModelS but not by Fastlim, and vice versa the green points. The up-plot corresponds to all the implemented analyses by both tools, while the down-plot shows only the common analyses implemented.

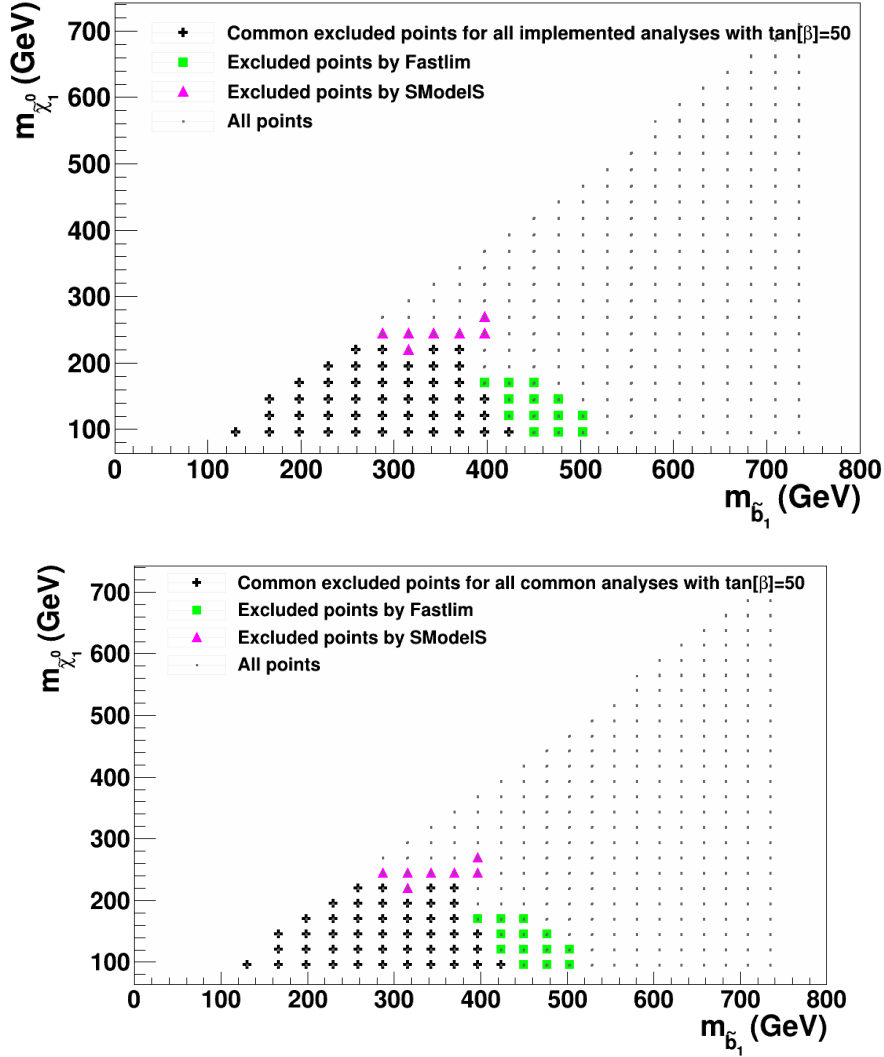


Figure 28: Left-handed bottom squark - LSP marginalized exclusion plot for $\tan\beta = 50$. The black points show the common excluded points between SModelS and Fastlim, the pink points show those excluded by SModelS but not by Fastlim, and vice versa the green points. The up-plot corresponds to all the implemented analyses by both tools, while the down-plot shows only the common analyses implemented.

References

- [1] ATLAS Collaboration. Atlas supersymmetry (susy) searches: Summary plots. https://twiki.cern.ch/twiki/bin/view/AtlasPublic/SupersymmetryPublicResults#Summary_plots_status_Moriond_201, 2014.
- [2] G. L. Kane, Chris Kolda, Leszek Roszkowski, and James D. Wells. Study of constrained minimal supersymmetry. *Phys. Rev. D*, 49:6173–6210, Jun 1994.
- [3] S Sekmen, S Kraml, J Lykken, F Moortgat, S Padhi, L Pape, M Pierini, HB Prosper, and M Spiropulu. Interpreting lhc susy searches in the phenomenological mssm. *Journal of High Energy Physics*, 2012(2):1–14, 2012.
- [4] Stephen P Martin. *A supersymmetry primer*, volume 1. World Scientific, Singapore, 2010.
- [5] Adrian Signer. Abc of susy. *arXiv preprint arXiv:0905.4630*, 2009.

- [6] Genesis Perez. Study of an electron-muon resonance in a r-parity violating supersymmetric model using atlfast-ii. Master's thesis, Lund University, 2012. <http://lup.lub.lu.se/luur/download?func=downloadFile&recordId=3045061&fileId=3045075>.
- [7] Sabine Kraml. Stop and sbottom phenomenology in the mssm. *arXiv preprint hep-ph/9903257*, 1999.
- [8] Michele Papucci, Joshua T Ruderman, and Andreas Weiler. Natural susy endures. *Journal of High Energy Physics*, 2012(9):1–45, 2012.
- [9] Sabine Kraml, Suchita Kulkarni, Ursula Laa, Andre Lessa, Wolfgang Magerl, Doris Proschofsky-Spindler, and Wolfgang Waltenberger. Smodels: a tool for interpreting simplified-model results from the lhc and its application to supersymmetry. *arXiv preprint arXiv:1312.4175*, 2013.
- [10] Daniele Alves, Nima Arkani-Hamed, Sanjay Arora, Yang Bai, Matthew Baumgart, Joshua Berger, Matthew Buckley, Bart Butler, Spencer Chang, Hsin-Chia Cheng, et al. Simplified models for lhc new physics searches. *Journal of Physics G: Nuclear and Particle Physics*, 39(10):105005, 2012.
- [11] Search for direct production of the top squark in the all-hadronic $t\bar{t} + \text{etmiss}$ final state in 21 fb-1 of p-p collisions at $\sqrt{s}=8$ TeV with the ATLAS detector. Technical Report ATLAS-CONF-2013-024, CERN, Geneva, Mar 2013.
- [12] Michele Papucci, Kazuki Sakurai, Andreas Weiler, and Lisa Zeune. Fastlim: a fast lhc limit calculator. *arXiv preprint arXiv:1402.0492*, 2014.
- [13] Suchita Kulkarni. Introducing smodels, October 2013. SModelS presented at the GDR terascale.
- [14] Kazuki Sakurai. Fastlim: a fast lhc limit calculator, July 2013. Fastlim presented at the LHC Physics Discussion SUSY at DESY.
- [15] Search for squarks and gluinos with the ATLAS detector in final states with jets and missing transverse momentum and 20.3 fb⁻¹ of $\sqrt{s} = 8$ TeV proton-proton collision data. Technical Report ATLAS-CONF-2013-047, CERN, Geneva, May 2013.
- [16] CMS collaboration et al. Interpretation of searches for supersymmetry with simplified models. *arXiv preprint arXiv:1301.2175*, 2013.
- [17] Search for direct top squark pair production in final states with one isolated lepton, jets, and missing transverse momentum in $\sqrt{s} = 8, \text{TeV}$ pp collisions using 21 fb⁻¹ of ATLAS data. Technical Report ATLAS-CONF-2013-037, CERN, Geneva, Mar 2013.
- [18] Search for direct third generation squark pair production in final states with missing transverse momentum and two b -jets in $\sqrt{s} = 8$ TeV pp collisions with the ATLAS detector. Technical Report ATLAS-CONF-2013-053, CERN, Geneva, May 2013.
- [19] Search for direct top squark pair production in final states with two leptons in $\sqrt{s} = 8$ TeV pp collisions using 20fb⁻¹ of ATLAS data. Technical Report ATLAS-CONF-2013-048, CERN, Geneva, May 2013. Not published in the proceedings.
- [20] Search for direct production of charginos and neutralinos in events with three leptons and missing transverse momentum in 21 fb⁻¹ of pp collisions at $\sqrt{s} = 8$ TeV with the ATLAS detector. Technical Report ATLAS-CONF-2013-035, CERN, Geneva, Mar 2013.
- [21] Search for chargino and neutralino production in final states with one lepton, two b -jets consistent with a Higgs boson, and missing transverse momentum with the ATLAS detector in 20.3 fb⁻¹ of $\sqrt{s} = 8$ TeV pp collisions. Technical Report ATLAS-CONF-2013-093, CERN, Geneva, Aug 2013.

- [22] Search for strong production of supersymmetric particles in final states with missing transverse momentum and at least three b-jets using 20.1 fb1 of pp collisions at $\sqrt{s} = 8$ TeV with the ATLAS Detector. Technical Report ATLAS-CONF-2013-061, CERN, Geneva, Jun 2013.
- [23] Search for direct-slepton and direct-chargino production in final states with two opposite-sign leptons, missing transverse momentum and no jets in 20/fb of pp collisions at $\sqrt{s} = 8$ TeV with the ATLAS detector. Technical Report ATLAS-CONF-2013-049, CERN, Geneva, May 2013.
- [24] Search for strongly produced superpartners in final states with two same sign leptons with the ATLAS detector using 21 fb-1 of proton-proton collisions at $\sqrt{s}=8$ TeV. Technical Report ATLAS-CONF-2013-007, CERN, Geneva, Mar 2013.
- [25] Georges Aad et al. Search for new phenomena in final states with large jet multiplicities and missing transverse momentum at $\sqrt{s}=8$ TeV proton-proton collisions using the ATLAS experiment. *JHEP*, 1310:130, 2013.
- [26] Search for Supersymmetry in final states with two same-sign leptons, jets and missing transverse momentum with the ATLAS detector in pp collisions at $\sqrt{s}=8$ TeV. Technical Report ATLAS-CONF-2012-105, CERN, Geneva, Aug 2012.
- [27] Search for strongly produced supersymmetric particles in decays with two leptons at $\sqrt{s} = 8$ TeV. Technical Report ATLAS-CONF-2013-089, CERN, Geneva, Aug 2013.
- [28] Search for squarks and gluinos in events with isolated leptons, jets and missing transverse momentum at $\sqrt{s} = 8$ TeV with the ATLAS detector. Technical Report ATLAS-CONF-2013-062, CERN, Geneva, Jun 2013.
- [29] Search for direct stop pair production in events with a Z boson, b-jets and missing transverse energy with the ATLAS detector using 21 fb⁻¹ from proton-proton collision at $\sqrt{s} = 8$ TeV. Technical Report ATLAS-CONF-2013-025, CERN, Geneva, Mar 2013.
- [30] Search for direct top squark pair production in final states with one isolated lepton, jets, and missing transverse momentum in $\sqrt{s} = 8$ TeV pp collisions using 13.0 ifb of ATLAS data. Technical Report ATLAS-CONF-2012-166, CERN, Geneva, Dec 2012.
- [31] Search for direct stop production in events with missing transverse momentum and two b-jets using 12.8 fb⁻¹ of pp collisions at $\sqrt{s} = 8$ TeV with the ATLAS detector. Technical Report ATLAS-CONF-2013-001, CERN, Geneva, Jan 2013.
- [32] Georges Aad et al. Search for direct third-generation squark pair production in final states with missing transverse momentum and two b-jets in $\sqrt{s} = 8$ TeV pp collisions with the ATLAS detector. *JHEP*, 1310:189, 2013.
- [33] Searches for direct scalar top pair production in final states with two leptons using the transverse mass variable and a multivariate analysis technique in $\sqrt{s} = 8$ TeV pp collisions using 20.3 fb⁻¹ of ATLAS data. Technical Report ATLAS-CONF-2013-065, CERN, Geneva, Jul 2013.
- [34] Search for supersymmetry in events with four or more leptons in 21 fb⁻¹ of pp collisions at $\sqrt{s} = 8$ TeV with the ATLAS detector. Technical Report ATLAS-CONF-2013-036, CERN, Geneva, Mar 2013.
- [35] Search for electroweak production of supersymmetric particles in final states with at least two hadronically decaying taus and missing transverse momentum with the ATLAS detector in proton-proton collisions at $\sqrt{s} = 8$ TeV. Technical Report ATLAS-CONF-2013-028, CERN, Geneva, Mar 2013.

- [36] A Search for Anomalous Production of Events with three or more leptons using 9.2fb. Technical Report CMS-PAS-SUS-12-026, CERN, Geneva, 2012.
- [37] Search for supersymmetry in pp collisions at $\sqrt{s} = 8$ TeV in events with three leptons and at least one b-tagged jet. Technical Report CMS-PAS-SUS-13-008, CERN, Geneva, 2013.
- [38] Search for supersymmetry using razor variables in events with b-jets in pp collisions at 8 TeV. Technical Report CMS-PAS-SUS-13-004, CERN, Geneva, 2013.
- [39] Search for gluino-mediated bottom- and top-squark production in pp collisions at 8 TeV. Technical Report CMS-PAS-SUS-12-024, CERN, Geneva, 2013.
- [40] Search for supersymmetry in pp collisions at $\sqrt{s} = 8$ TeV in events with two opposite sign leptons, large number of jets, b-tagged jets, and large missing transverse energy. Technical Report CMS-PAS-SUS-13-016, CERN, Geneva, 2013.
- [41] Search for supersymmetry in final states with missing transverse energy and 0, 1, 2, 3, or at least 4 b-quark jets in 8 TeV pp collisions using the variable AlphaT . Technical Report CMS-PAS-SUS-12-028, CERN, Geneva, 2012.
- [42] Search for New Physics in the Multijets and Missing Momentum Final State in Proton-Proton Collisions at 8 TeV. Technical Report CMS-PAS-SUS-13-012, CERN, Geneva, 2013.
- [43] Search for new physics in events with same-sign dileptons and jets in pp collisions at 8 TeV. Technical Report CMS-PAS-SUS-13-013, CERN, Geneva, 2013.
- [44] A search for anomalous production of events with three or more leptons using 19.5/fb of $\sqrt{s}=8$ TeV LHC data. Technical Report CMS-PAS-SUS-13-002, CERN, Geneva, 2013.
- [45] Search for Supersymmetry in pp collisions at 8 TeV in events with a single lepton, multiple jets and b-tags. Technical Report CMS-PAS-SUS-13-007, CERN, Geneva, Mar 2013.
- [46] Search for top-squark pair production in the single lepton final state in pp collisions at 8 TeV. Technical Report CMS-PAS-SUS-13-011, CERN, Geneva, 2013.
- [47] Search for direct EWK production of SUSY particles in multilepton modes with 8TeV data. Technical Report CMS-PAS-SUS-12-022, CERN, Geneva, 2013.
- [48] Search for electroweak production of charginos, neutralinos, and sleptons using leptonic final states in pp collisions at 8 TeV. Technical Report CMS-PAS-SUS-13-006, CERN, Geneva, 2013.
- [49] Search strategy for exclusive multi-jet events from supersymmetry at CMS. Technical Report CMS-PAS-SUS-09-001, CERN, 2009. Geneva, Jul 2009.
- [50] Search for new phenomena using final states with large jet multiplicities and missing transverse momentum with ATLAS in 20 fb^{-1} of $\sqrt{s} = 8$ TeV proton-proton collisions. Technical Report ATLAS-CONF-2013-054, CERN, Geneva, May 2013.